

## IV. MEDIUM-ENERGY NUCLEAR PHYSICS RESEARCH

### OVERVIEW

In order to test our understanding of the structure of hadrons and the structure of nuclei within the framework of quantum chromodynamics, the medium-energy research program in the Argonne Physics Division emphasizes study of nucleons and nuclei on a relatively short distance scale. In particular, related physics topics are examined at both the quark and hadronic levels in order to understand the non-perturbative nature of strong interactions. Because the electromagnetic interaction provides an accurate, well-understood probe of these phenomena, primary emphasis is placed on experiments involving electron scattering, real photons and Drell-Yan processes.

The electron beams of the Thomas Jefferson National Accelerator Facility (TJNAF) are ideally suited for studies of nuclei at hadronic scales and represent one center of the experimental program. Staff members led in the construction of experimental facilities, serve as spokespersons or co-spokepersons for 12 experiments and are actively involved in several others. The group constructed the broad-purpose Short Orbit Spectrometer which forms half of the coincidence spectrometer pair that is the base experimental equipment in Hall C. We continue to upgrade the SOS detector package and improve the understanding of the spectrometer optics and acceptance. Argonne led the first experiment to be carried out at TJNAF in FY1996 and has completed nine other experiments. In FY1999 measurements were made with a 5.5 GeV electron beam to extend our results on the  $d(\gamma,p)n$  and  $(e,e'p)$  reactions to higher scales. An experiment was also completed to measure the ratio of the longitudinal to transverse inelastic electron scattering response in the resonance region. We also measured kaon electroproduction on targets of  $^3\text{He}$  and  $^4\text{He}$  to study the reaction mechanism of electroproduction of hypernuclei and to search for bound  $\Sigma$ -hypernuclear states. Now these experiments are undergoing analysis. Also, during the past year, the group prepared to measure the  $\pi^-/\pi^+$  ratio in high-energy photodisintegration of the deuteron in Hall A at TJNAF.

The first results from TJNAF build upon previous ANL experiments at Stanford Linear Accelerator Center (SLAC), MIT-Bates and Saclay (ALS). For the first time, forward-backward angle measurements of the  $(e,e'p)$  reaction have been used to perform longitudinal-transverse separations of the proton spectral function at high momentum transfers. Exclusive deuteron photodisintegration experiments have established that this reaction obeys quark-counting-rule scaling arguments at large transverse momenta. The extension of this work to 5.5 GeV indicates that

the forward-angle deuteron photodisintegration cross section is consistent with the quark counting rules. In addition, polarization measurements for exclusive deuteron photodisintegration indicate a remarkable departure from the meson-nucleon picture. Measurements of kaon production on hydrogen, deuterium,  $^3\text{He}$  and  $^4\text{He}$  provide important information on the basic strangeness production mechanisms, the poorly known low energy hyperon-nucleon interaction and the electromagnetic form factor of the  $K^+$ . Pion production measurements on hydrogen, deuterium,  $^3\text{He}$  and  $^4\text{He}$  will determine the charge form factor of the pion and measure the change in the pion field in the nuclear medium. Since the pion contains valence antiquarks, these measurements complement our high-energy Drell-Yan measurements of the antiquark distributions in nucleons and nuclei. Results of new measurements of inclusive electron scattering in the resonance region provide evidence for the concept of semi-local duality in relating averaged resonance and deep inelastic scattering yields.

HERMES, a broadly based North American-European collaboration is studying the spin structure of the nucleon using internal polarized targets in the HERA storage ring at DESY. Deep inelastic scattering has been measured with polarized electrons on polarized hydrogen, deuterium and  $^3\text{He}$ . Argonne has concentrated on the hadron particle identification of HERMES, a unique capability compared to other spin structure experiments. In 1999 and under Argonne leadership, the dual-radiator ring imaging Cerenkov counter (RICH) was brought into operation at the design specifications to provide complete hadron identification in the experiment. The RICH has been operating routinely since its installation. This will allow HERMES to make decisive measurements of the flavor dependence of the spin distributions. HERMES made the first direct measurement of the spin dependence of the glue in the photoproduction of pairs of high transverse momenta pions. The HERMES experiment is also making significant advances in unpolarized deep-inelastic scattering physics with its coincident hadron detection. Argonne scientists have extended the physics program in studies of exclusive vector meson production in polarized-beam-polarized-target measurements and also measurements on nuclear targets. Clear evidence is seen on the nuclear targets for the effect of coherence in the production mechanism. An unexpected strong nuclear dependence of the ratio of longitudinal to transverse deep inelastic scattering cross sections has been observed at low  $x$  and  $Q^2$ . This was explored further in a TJNAF experiment during 2000.

Recently, a single-spin asymmetry in the azimuthal distribution of  $\pi^+$  was observed from a longitudinally polarized proton target. This new result will render transversity measurements feasible at HERMES. In addition, HERMES observed the deeply virtual Compton scattering process which is an important tool for investigating the structure of the proton.

Measurements of high mass virtual photon production in high-energy proton-induced reactions have determined the flavor dependence of the sea of antiquarks in the nucleon. These measurements give insight into the origin of the nucleon sea. In the same experiment, the nuclear dependence of the Drell-Yan process and the nuclear dependence of the production of heavy quark resonances such as the  $J/\psi$  and  $\Upsilon$  have been determined. The Drell-Yan results demonstrate that the energy loss of quarks in the nuclear medium is significantly less than theoretical expectations. The heavy vector meson results provide constraints on the gluon distributions of nucleons and nuclei and a significant baseline for attempts to use heavy vector meson production as a signal of the formation of the quark-gluon

plasma in relativistic heavy-ion experiments. A new initiative is underway to continue these measurements with much higher luminosity at the FNAL Main Injector.

The technology of laser atom traps provides a unique environment for the study of nuclear and atomic systems and represents a new thrust for the group. Initially the efforts focus on developing high efficiency and high sensitivity trapping techniques for the isotope analysis of noble gases. The isotope Krypton-81 was detected at natural ( $10^{-13}$ ) abundance and the technique was demonstrated to be free of contamination from other isotopes and elements. This atom trace analysis (ATTA) technique provides a new approach to such diverse problems as dating old ground water or mapping out the atmospheric concentration of fission products. Work has begun on applying ATTA to the detection of  $^{41}\text{Ca}$ . As a necessary step in this direction,  $^{40}\text{Ca}$  was successfully trapped. In addition, the charge radius of  $^6\text{He}$  is being investigated.

## A. SUBNUCLEONIC EFFECTS IN NUCLEI

### a.1. New Measurement of ( $G_E/G_M$ ) For the Proton (J. Arrington, F. Dohrmann, D. Gaskell, D. F. Geesaman, K. Hafidi, R. J. Holt, H. E. Jackson, D. H. Potterveld, P. E. Reimer, K. Wijesooriya, and B. Zeidman, and the E01-001 Collaboration)

The structure of the proton is a matter of universal interest in nuclear and particle physics. Charge and current distributions are obtained through measurements of the electric and magnetic form factors,  $G_E(Q^2)$  and  $G_M(Q^2)$ . These form factors can be separated by measuring elastic electron-proton scattering at two or more values of the virtual photon polarization parameter  $\varepsilon$  (*i.e.* by performing Rosenbluth global fits to these measurements indicated that the form factors were consistent with the dipole form, and that the ratio of  $G_E$  to  $G_M$  was consistent with unity. However these measurements are difficult at large values of  $Q^2$  where the cross section is dominated by the magnetic form factor, and while none of the experiments were inconsistent with a constant value of  $G_E/G_M$ , the agreement between the experiments was rather poor (as shown in Fig. IV-1).

Recent measurements at Jefferson Laboratory<sup>1</sup> used a polarization transfer measurement to extract  $G_E/G_M$  at large values of  $Q^2$ . They found that the ratio of  $\mu G_E/G_M$  was unity at low  $Q^2$ , but fell linearly with increasing  $Q^2$ , reaching a value of 0.6 at  $Q^2 = 3 \text{ GeV}^2$ .

While this new technique can reach higher values of  $Q^2$  and is less prone to systematic uncertainties than the Rosenbluth separation, the discrepancy between the two techniques must be understood before we can be comfortable accepting the results of either set of experiments.

Experiment E01-001 will perform a Rosenbluth separation to measure  $G_E/G_M$  at  $Q^2 = 1.4, 3.2, \text{ and } 4.9 \text{ GeV}^2$ , but will use a different experimental technique that will reduce the uncertainty compared to previous measurements. To measure at two different values of  $\varepsilon$ , data must be taken at different beam energies and different electron scattering angles. In order to extract the small contribution from  $G_E$ , the uncertainty in the ratio of high- $\varepsilon$  to low- $\varepsilon$  data must be extremely small. Uncertainties in the accumulated beam charge, target density, and scattering kinematics are some of the most significant sources of uncertainty in the previous measurements. To reduce the dependence on beam charge and target density, we will make simultaneous measurements at the desired (high)  $Q^2$  value and a low  $Q^2$  normalization point ( $0.5 \text{ GeV}^2$ ).

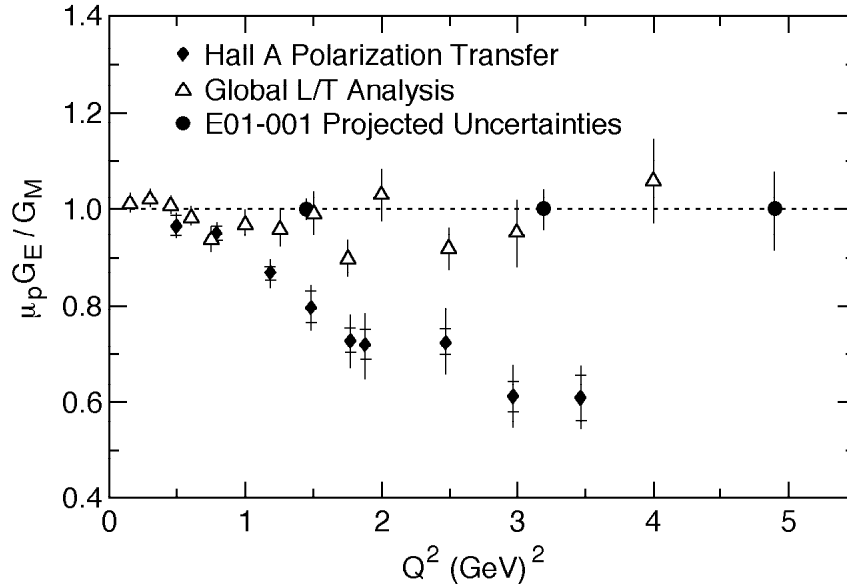


Fig. IV-1. Existing measurements of  $G_E/G_M$ , along with projected uncertainties for this experiment. The hollow points represent the results from Rosenbluth separation experiments, while the solid stars represent the recent Hall A polarization transfer measurement.

Because the value of  $G_E/G_M$  at low  $Q^2$  is relatively well known, and because the kinematics chosen make the low  $Q^2$  measurement insensitive to the photon polarization, we can use the low  $Q^2$  point to correct for any error in the beam charge and target thickness measurements. The other difference in this measurement is that we will detect the struck proton, rather than the scattered electron. This significantly reduces the sensitivity to the scattering angle for the forward angle electron scattering (large angle proton scattering) where it is a significant contribution to the uncertainty. It also increases the cross section for backwards angle electrons (forwards angle protons), where the cross section becomes a limiting factor in the electron measurement. The proton also has the advantage that the radiative corrections are both smaller than in the electron case, and less dependent on  $\epsilon$ .

Finally, because the proton momentum is fixed for a given  $Q^2$ , the detected particle is at the same momentum for both the forward and backward angle measurements, reducing the uncertainty from any momentum-dependent corrections to the cross section.

The experiment was approved<sup>2</sup> for 10 days of beam time in Hall A at Jefferson Lab. The uncertainty in the extraction of the ratio depends on the value of  $G_E/G_M$ . Assuming form factor scaling ( $G_E/G_M = 1$  at all  $Q^2$ ), the uncertainty on the ratio is 2.1% at  $Q^2 = 1.4$  GeV<sup>2</sup>, 4.2% at  $3.2$  GeV<sup>2</sup>, and 9.7% at  $4.9$  GeV<sup>2</sup>. This experiment will differentiate between the existing Rosenbluth data and the new polarization transfer results up to  $Q^2 = 5$  GeV<sup>2</sup> and will give the most precise measurement of  $G_E/G_M$  at moderate  $Q^2$ .

<sup>1</sup>M. K. Jones et al., Phys. Rev. Lett. **84**, 1398 (2000).

<sup>2</sup>J. Arrington, R. E. Segel et al., Jlab Experiment E01-001.

**a.2. The Energy Dependence of Nucleon Propagation in Nuclei as Measured in the (e,e'p) Reaction** (D. F. Geesaman, J. Arrington, K. Bailey, W. J. Cummings, D. DeSchepper, R. Holt, H. E. Jackson, C. Jones, S. Kaufman, T. O'Neill, D. Potterveld, J. Reinhold, J. P. Schiffer, and B. Zeidman, and the E91-013 and E94-139 Collaborations)

ANL led the first experiment to be carried out at TJNAF in 1995-1996. This experiment built upon earlier ANL work at MIT and SLAC using the (e,e'p) reaction to study the propagation of 0.35-3.3 GeV protons through nuclear material and the reaction mechanism in the quasifree region. Measurements were made at  $Q^2$  values of 0.64, 1.3, 1.8 and 3.3  $\text{GeV}^2$ . At  $Q^2$  of 0.64 and 1.8  $\text{GeV}^2$  data were taken at two values of the virtual photon polarization to examine the separate contributions of longitudinal and transverse photon exchange. The statistics, kinematic coverage and experimental precision significantly exceed those of previous measurements. These data provide precise measurements of nuclear transparency as well as a broad survey of nuclear spectral functions from recoil momentum of 0 to 300 MeV and missing energy of 0 to 150 MeV.

Radiatively corrected spectral functions have been extracted for each target and momentum transfer. These spectral functions suggest that the widths of deeply bound hole states in Fe and Au may be somewhat larger than had been expected. Separated longitudinal and transverse spectral functions were extracted for missing momenta from 0 to 80 MeV at two  $Q^2$  values. At  $Q^2 = 1.8 \text{ GeV}^2$ , the longitudinal and

transverse spectral functions of the s-shell and p-shell knockout strength are consistent with each other. However, at  $Q^2$  of 0.6  $\text{GeV}^2$ , there is a substantial excess of transverse strength compared to the longitudinal strength in the missing energy region from 30-50 MeV. Similar results are observed for iron and gold. The missing energy and nucleus dependence suggest that meson exchange mechanisms are important for the transverse strength, especially at the lower  $Q^2$ . The longitudinal strength is observed to extend to the highest missing energies measured signaling the effects of short-range correlations.

Additional measurements were made in 1999, significantly extending the momentum transfer coverage of the nuclear transparency measurement. Data were taken on deuterium, carbon, and iron up to  $Q^2 = 8.0 \text{ GeV}^2$ . Figure IV-2 shows the measured transparency for both JLab experiments, as well as previous measurements from MIT-Bates and SLAC. The JLab data extends somewhat higher in  $Q^2$  than the previous SLAC measurements, with significantly smaller uncertainties. These new results rule out large color transparency effects at these values of momentum transfer.

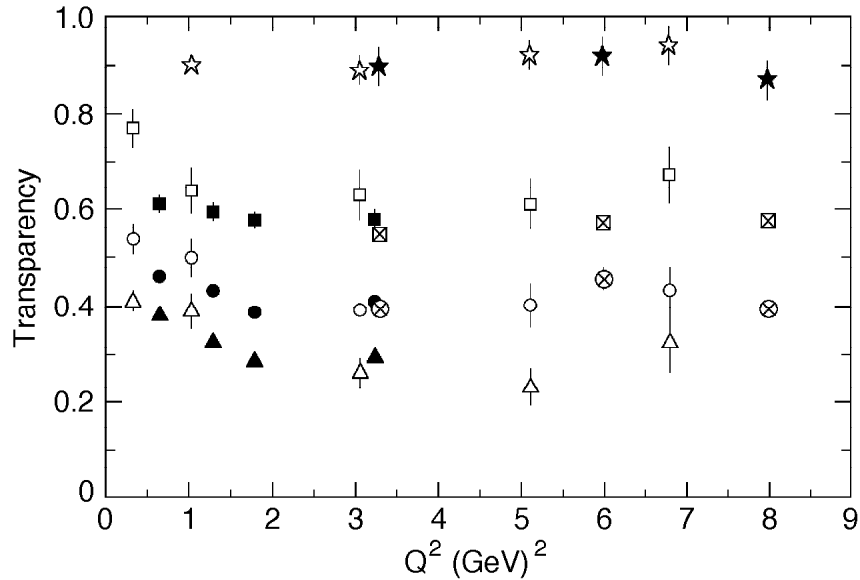


Figure IV-2. Nuclear transparency from JLab experiments E91-003 and E94-139 (solid symbols), along with previous measurements from SLAC and Bates (hollow symbols). Data is shown for deuterium (stars), carbon (squares), iron (circles), and gold (triangles).

### a.3. Measurements of $R = \sigma_L / \sigma_T$ in the Nucleon Resonance Region (J. Arrington, D. F. Geesaman, T. G. O'Neill, and D. Potterveld, and the E99-119 Collaboration)

A great deal of our understanding of the quark structure of the nucleon comes from inclusive electron scattering. However, most of the measurements focus on the deep inelastic region. High precision cross section measurements in the resonance region, combined with a separation of the longitudinal ( $\sigma_L$ ) and transverse ( $\sigma_T$ ) components, will substantially improve the global description of electroproduction at moderate to high  $Q^2$  and large Bjorken- $x$ . While the ratio  $R = \sigma_L / \sigma_T$  has been measured up to high  $Q^2$  for elastic and deep inelastic scattering, there exist few

measurements of  $R$  in the resonance region at moderate or high momentum transfers.

In 1999, experiment E94-110 was run in Hall C at Jefferson Lab. The experiment made a precision measurement of  $R$  in the resonance region, up to  $Q^2 = 4.5 \text{ GeV}^2$ . This new data should reduce the uncertainty in  $R$  from greater than 100% to approximately 10%. There is also an additional approved experiment to extend duality studies to  $Q^2 = 7.5 \text{ GeV}^2$ .

### a.4. Measurement of Proton Polarization in Neutral Pion Photoproduction (R. J. Holt, C. Schulte, and K. Wijesooriya and the Hall A Collaboration)

There are two tests of perturbative Quantum Chromodynamics (pQCD) in exclusive nuclear reactions: i) whether the reaction obeys the constituent counting rules, and ii) whether hadron helicity is conserved. Existing cross section data for  $H(\gamma, \pi^+)n$

reaction exhibit an energy dependence near  $\theta = 90^\circ$  consistent with asymptotic scaling for photon energies above 2 GeV. However, attempts to observe Hadron Helicity Conservation (HHC) are believed to be obscured by the presence of Landshoff amplitudes

which appear in hadron-hadron collisions but not in photo reactions. The  $H(\gamma, \bar{p})\pi^0$  reaction is an excellent candidate for testing HHC not only because it has no Landshoff corrections, but also it involves a relatively small number of constituents and only two helicity amplitudes.

Jefferson Lab experiment E94-012, measured spin observables both across much of the resonance region ( $E_\gamma \approx 0.8\text{--}2.0$  GeV), and up to much higher energies ( $E_\gamma = 4.8$  GeV) at center of mass angles between  $45^\circ$  and  $120^\circ$ . The induced polarization,  $P_y$  and polarization transfer coefficients,  $C_x$  and  $C_z$  were

measured for the  $\gamma p \rightarrow p\pi^0$  reaction using a circularly polarized bremsstrahlung beam and the Hall A focal plane polarimeter in the hadron spectrometer. The electron spectrometer was used to tag the electron from the ep elastic scattering to veto the elastics. The preliminary results for the induced polarization,  $P_y$  at 856 MeV photon energy agree well with the available world data and also agrees qualitatively with the SAID prediction. There are no data available for the polarization transfer observables for this reaction prior to this experiment.

**a.5. Two-Body Photodisintegration of the Deuteron Up to 5.5 GeV (R. J. Holt, J. Arrington, D. F. Geesaman, H. E. Jackson, T. O'Neill, D. H. Potterveld, E. C. Schulte, and B. Zeidman, and the E96-003 Collaboration)**

The overall goal of experiment E96-003 is to map out the transition region from a nucleon-meson picture of deuteron photodisintegration to the quark-gluon picture. High energy two-body breakup of the deuteron is an excellent means to probe quark effects in nuclear reactions since the energy transfer to the constituents is large. Previous experiments at JLab were limited to 4.0 GeV. Although these experiments found evidence for scaling at reaction angles near  $90^\circ$ , no evidence for scaling was found at forward angles. The objective of E96-003 is to extend the cross section measurements for the  $d(\gamma, p)n$  reaction up to a photon energy of 5.5 GeV at forward angles as a test for scaling at the forward angles. The HMS in Hall C was used to detect

photoprotons which emerged from a liquid deuterium target that was irradiated by bremsstrahlung photons.

Relatively large momentum transfer<sup>1</sup> to the constituents can be obtained in exclusive photonuclear reactions at photon energies of a few GeV, because the absorbed photon delivers all of its energy to the constituents. One signature of a QCD effect in the  $d(\gamma, p)n$  reaction is a scaling behavior, for example, the constituent counting rule behavior. For deuteron photodisintegration  $\gamma d \rightarrow pn$  process, the constituent counting rule<sup>2</sup> predicts:

$$\frac{d\sigma}{dt} \propto s^{-11}.$$

<sup>1</sup>R. J. Holt, Phys. Rev. C **41**, 2400 (1990).

<sup>2</sup>S. J. Brodsky and G. R. Farrar, Phys. Rev. Lett. **31**, 1153 (1973); G. P. Lepage and S. J. Brodsky, Phys. Rev. D. **22**, 2157 (1980); V. Matveev *et al.*, Nuovo Cimento Lett. **7**, 719 (1973).

<sup>3</sup>C. Bochna *et al.*, Phys. Rev. Lett. **81**, 4576 (1998).

<sup>4</sup>J. Arends *et al.*, Nucl. Phys. A **412**, 509 (1984); J. E. Belz *et al.*, Phys. Rev. Lett. **74**, 646 (1995); R. Ching and C. Schaerf, Phys. Rev. **141**, 1320 (1966); R. Crawford *et al.*, Nucl. Phys. A **603**, 281 (1996); P. Dougan *et al.*, Z. Phys. A **276**, 55 (1976); H. Myers *et al.*, Phys. Rev. **121**, 630 (1961); J. Napolitano *et al.*, Phys. Rev. Lett. **61**, 2530 (1988);

S. J. Freedman *et al.*, Phys. Rev. C **48**, 1864 (1993).

<sup>5</sup>T.-S. H. Lee, Argonne National Laboratory Report No. PHY-5253-TH-88; T.-S.H. Lee, in *Proceedings of the International Conference on Medium and High Energy Nuclear Physics, Taipei, Taiwan, 1988* (World Scientific, Singapore, 1988), p. 563.

<sup>6</sup>L. L. Frankfurt *et al.*, Phys. Rev. Lett. **84**, 3045 (2000).

This behavior has been observed at large angles,  $\theta_{cm} = 70$  and  $90^\circ$  as shown in Figure IV-3. Here,  $s^{11}d\sigma/dt$  is plotted as a function of  $E_\gamma$ . The new results shown as the diamonds in the figure are from experiment E96-003. These results indicate the first evidence for scaling at the forward angles and the highest energies. At  $53^\circ$  it appears that scaling sets in at photon energy of about 3 GeV, whereas at  $37^\circ$  there is the suggestion of scaling at 4 GeV. Because of the relatively large error limits and the relatively small energy region of the

experiment, scaling cannot be claimed conclusively. An additional experiment which goes to higher energy would be necessary to confirm this surprising result. The quark rescattering model<sup>6</sup> at the highest energy and especially at  $\theta_{cm} = 53^\circ$  is not in good agreement with the new data. Nevertheless, evidence for scaling at all the angles suggests that the GeV region is a “transition region” between meson-exchange models and pQCD. The experiment was completed, the data were analyzed and a manuscript is being prepared.

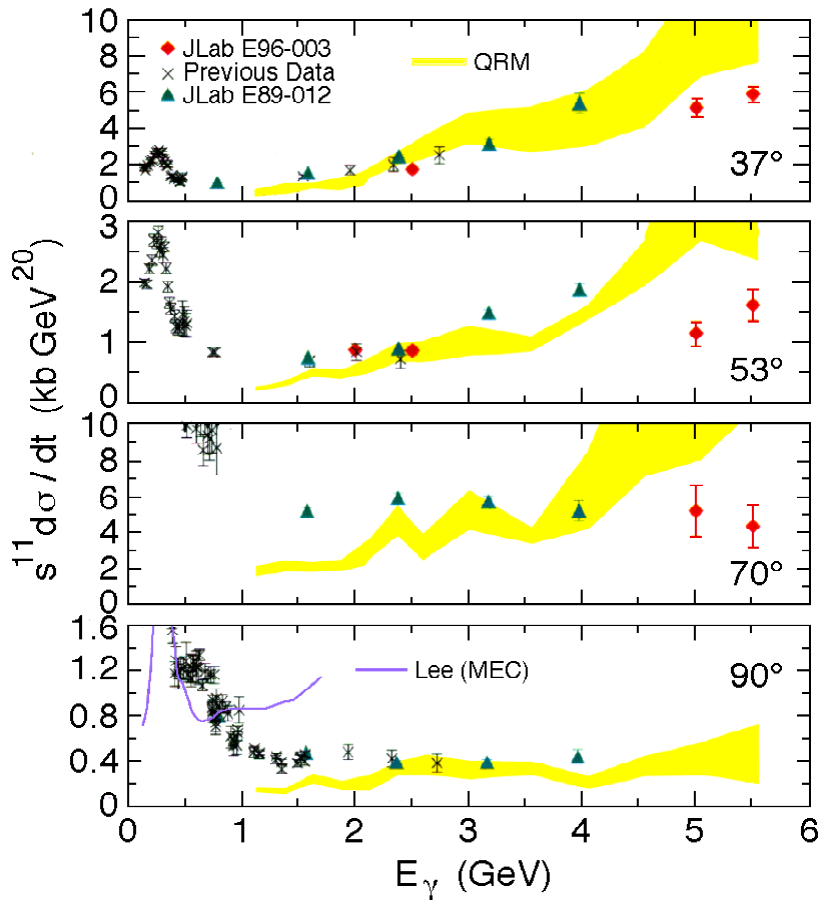


Figure IV-3. Data for deuteron photodisintegration as a function of the photon energy at four reaction angles. The darkened diamonds represent the E96-003 data. The darkened triangles represent the JLab E89-012 data.<sup>3</sup> The crosses are all the other existing data.<sup>4</sup> The solid line is a traditional meson-exchange calculation,<sup>5</sup> and the shaded area is the quark rescattering model.<sup>6</sup> These models have an absolute normalization. For the first time, evidence for scaling is observed at the forward reaction angles.



### a.6. Measurement of Proton Polarization in Deuteron Photodisintegration (R. J. Holt, E. C. Schulte, and K. Wijesooriya and the Hall A Collaboration)

There are two distinct classes of calculations to describe nuclear reactions. The Meson Exchange Calculations (MEC) that work very well in low energies and the perturbative Quantum Chromodynamic (pQCD) calculations that are expected to work well at very high energies. The main goal of this experiment is to see the applicability of these models in the intermediate energy regime, or to study the transition from the meson baryon picture to the quark gluon picture.

Cross section data for the  $d(\gamma,p)n$  reaction at  $\theta_{\text{cm}} = 90^\circ$  and photon energies above 1 GeV exhibit an  $s^{-11}$  scaling behavior that is consistent with MEC, pQCD and a nonperturbative QCD model. For this reason, we now provide a stringent test of these competing pictures of deuteron photodisintegration. Hall A, Jefferson Lab experiment E89-019 used polarized electrons with a 6% thick Cu radiator on 15 cm thick LD2 target and used the high resolution hadron spectrometer to detect the

recoiling proton. A Focal Plane polarimeter was used to determine the proton polarizations at the focal plane in addition to the standard detector package. Three polarization observables were measured: Induced polarization ( $p_y$ ), and the two polarization transfer observables,  $C_x$  and  $C_z$  for photon energies 0.5 GeV to 2.5 GeV.

As shown by the data in Fig. IV-4(a), the induced polarization,  $p_y$  vanishes above 1 GeV contrary to MEC, in which resonances lead to large polarizations showing a breakdown of the meson-baryon picture, but agreeing well with the pQCD prediction. However, polarization transfer  $C_x$  [see Fig. IV-4(b)] does not vanish above 1 GeV, inconsistent with the hadron helicity conservation expected from the pQCD picture, suggesting that the underlying picture in the intermediate energies is neither a MEC or pQCD, but rather a nonperturbative quark picture.

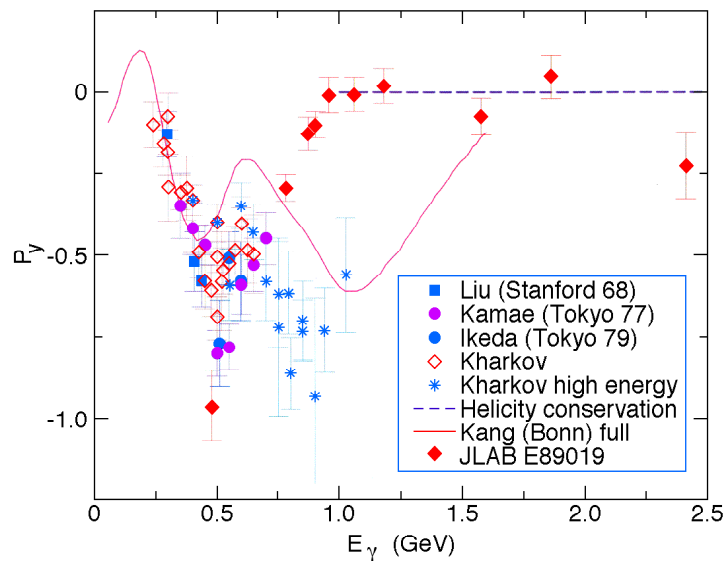
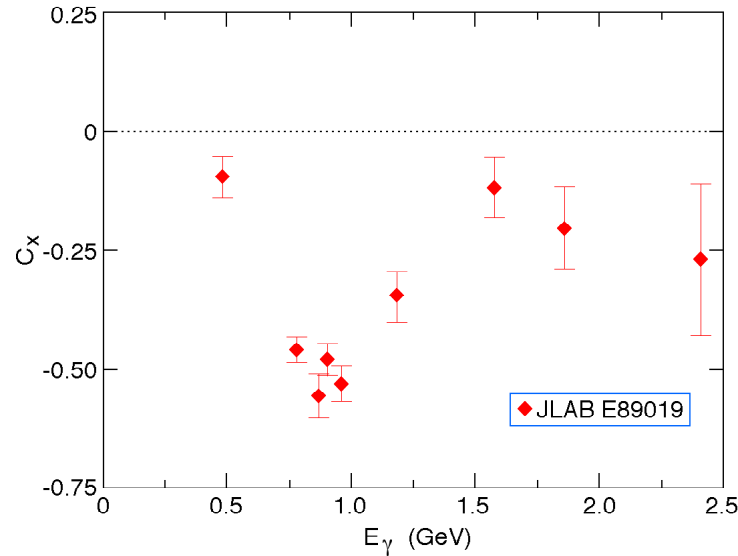


Figure IV-4. (a)



(b)

Figure IV-4: Polarization observables measured in deuteron photodisintegration at  $\theta_{cm} = 90^\circ$ . Induced polarization,  $p_y$  (polarization transfer,  $C_x$ ) in a (b).

#### a.7. Angular Distribution of the $\gamma d \rightarrow pn$ Reaction (R. J. Holt, E. C. Schulte, and K. Wijesooriya, and the E99-008 Collaboration)

The overall goal of experiment E99-008 is to determine the mechanism which governs photoreactions in the GeV energy region. If the incoming photon couples to a quark, then one would expect<sup>1</sup> the angular distribution for the  $d(\gamma,p)n$  reaction to be symmetric about  $90^\circ$ . However, if the photon couples to a nucleon, then one would expect<sup>2,3</sup> that the differential cross section in the forward direction to be substantially larger than in the backward direction. Previous

measurements<sup>4</sup> extend only to a photon energy of 1.6 GeV. The previous data are consistent with the meson-nucleon picture rather than the quark-gluon models. For the present experiment, the angular distribution was measured from  $\theta_{cm} = 30^\circ$  to  $153^\circ$  at photon energies between 0.8 and 2.5 GeV. The high resolution spectrometer in Hall A was used to detect photoprotons which emerged from a liquid deuterium target that was irradiated by bremsstrahlung photons. Presently, the data are being analyzed.

<sup>1</sup>S. J. Brodsky and J. R. Hiller, Phys. Rev. C **28**, 475 (1983).

<sup>2</sup>T.-S. H. Lee, Argonne National Laboratory Report No. PHY-5253-TH-88; T.-S.H. Lee, in *Proceedings of the International Conference on Medium and High Energy Nuclear Physics, Taipei, Taiwan, 1988* (World Scientific, Singapore, 1988), p.563.

<sup>3</sup>S. I. Nagorny, Yu. A. Kasatkin, and I.K. Kirichenko, Sov. J. Nucl. Phys. **55**, 189 (1992).

<sup>4</sup>S. J. Freedman *et al.*, Phys. Rev. C **48**, 1864 (1993).

**a.8. High Energy Pion Photoproduction From the Proton and Deuteron**

(R. J. Holt, J. Arrington, K. Bailey, P. E. Reimer, F. Dohrmann, K. Hafidi, T. O'Connor, E. C. Schulte, and K. Wijesooriya, and the E94-104 Collaboration)

The goal of experiment E94-104 is to determine the mechanism that governs high-energy photoreactions by focusing on photopion production from the nucleon. The central objective of the experiment is to measure the  $\pi^-/\pi^+$  ratio from the deuterium target. The prediction<sup>1</sup> of the meson exchange model would give a ratio near unity at  $\theta_{cm} = 90^\circ$ , while quark models can deviate substantially from this value. Another objective of the experiment is to measure the angular distribution as a function of energy for the  $\gamma p \rightarrow \pi^+ n$  and the  $\gamma n \rightarrow \pi^- p$

reactions. The experiment is in progress in Hall A at this time. The photon energies will range between 1.17 and 5.6 GeV and data will be taken for angles near  $\theta_{cm} = 90^\circ$ . The high resolution spectrometer (HRS) in Hall A is used to detect photopions which emerge from a liquid hydrogen and deuterium targets that is irradiated by bremsstrahlung photons. We expect that the data collection phase of the experiment to be completed by April 2001.

<sup>1</sup>T.-S. H. Lee, priv. comm. (2001).

**a.9. A Study of Longitudinal Charged-Pion Electroproduction in D, <sup>3</sup>He, and <sup>4</sup>He**

(H. E. Jackson, J. Arrington, K. Bailey, D. DeSchepper, D. Gaskell, D. F. Geesaman, B. Mueller, T. G. O'Neill, D. H. Potterveld, J. Reinhold, and B. Zeidman, and the E91-003 Collaboration)

According to the simplest models of the nucleon-nucleon force, pion-exchange currents in nuclei should give rise to a mass-dependent enhancement of the nuclear pion charge distribution. Longitudinal pion electroproduction should be sensitive to nuclear pion currents because of the dominance of the pion-pole process for charged-pion emission in the direction of the virtual photon. If current conceptions of pion-exchange currents in nuclei are correct, longitudinal electroproduction will be suppressed at lower momentum transfers and enhanced at higher momentum transfers. These currents should also manifest themselves in quark-antiquark distribution functions as observed in deep-inelastic scattering (DIS) on nuclei. However, analysis of parton distribution functions shows no evidence for any mass enhancements of sea quarks. Recent data from Drell-Yan studies which probe directly the quark-antiquark sea, show no mass dependence. These results suggest that a reformulation of pion-exchange models of the medium- and short-range properties of nuclear forces may be required. In an attempt to probe exchange currents directly, we have carried out a series of measurements of single-charged-pion electroproduction on the proton, deuteron, and <sup>3</sup>He at TJNAF. The goal is to measure the longitudinal cross section in parallel kinematics by means of a Rosenbluth separation, and to

search for target-mass dependent effects. The results from these measurements should provide insight into the absence of any enhancement of sea quark distributions in nuclei as measured in DIS.

The experiment, E91-003, was approved for an initial phase of 500 hours to make measurements at two kinematic configurations for four targets, H, <sup>2</sup>H, <sup>3</sup>He, and <sup>4</sup>He. Because the shakedown and commissioning of the Hall C cryogenic target proved much more difficult than anticipated, only a portion of this program was completed, but enough data was obtained with <sup>2</sup>H and <sup>3</sup>He to provide a useful examination of the mass dependence of the longitudinal cross sections. The measurements were carried out at Jefferson Lab in February-April 1998 using the Hall C facility. 0.845 to 3.245 GeV electrons were scattered from high-density cryo-targets. The scattered electrons were observed in the High Momentum Spectrometer in coincidence with pions observed in a short orbit spectrometer. The kinematic conditions correspond to momentum transfers for which, in one case, the electroproduction is expected to be quenched ( $K_\pi \approx 0.200$  GeV/c), and a second, in which according to the standard pion-exchange model of nuclear forces, one expects a substantial enhancement ( $K_\pi \approx 0.400$  GeV/c). Measurements were made at kinematics corresponding to two virtual photon polarizations for each momentum

transfer in order to use the data to carry out a Rosenbluth separation of the transverse and longitudinal cross sections.

The general features of the deuterium and  $^3\text{He}$  pion spectra in missing mass, are typical of quasifree scattering. The forward angle electroproduction cross section integrated over missing mass,

$$d^3\sigma / d\omega d\Omega_e d\Omega_\pi = \int \Gamma_\nu [d^2\sigma_t / dM d\Omega_\pi + \epsilon d^2\sigma_l / dM d\Omega_\pi] dM$$

provides the most direct basis for comparing quasifree electroproduction with production on the free nucleon. The ratio of this cross section to that of the proton is a robust indicator of any mass dependence. Measurements of absolute cross sections are not necessary, and to first order, corrections for decay-in-flight cancel in the ratio. To extract this quantity, the experimental measured coincidence yield is simulated in a Monte Carlo calculation (SIMC) using a realistic model of the experiment. The effects of spectrometer response, radiation, nucleon Fermi motion, and kinematic variation of the primary nucleon cross section are included in the simulation. The measured data are compared with the simulation. The input data are refined and the process iterated until the best fit is obtained. The extracted experimental cross section is then defined as

$$\sigma(Q_0^2, W_0, \Theta_{\text{cm}}) = \sigma_{\text{model}}(Q_0^2, W_0, \Theta_{\text{cm}}) \times (\text{data}) / (\text{SIMC}).$$

The resulting extracted cross section ratios are shown in Fig. IV-5.

Within the precision of the measurements there is no indication of multinucleon contributions. The measured values of the d ratios cluster around one, with the exception of the point for  $^3\text{He}$  at 0.197 GeV. There is no evidence in these data for a measurable enhancement of  $d\sigma_l/d\Omega_\pi$  in either target. The quenching observed in earlier measurements<sup>6</sup> on the deuteron at  $k_\pi = 0.2$  GeV is present in the deuteron data for  $W = 1.6$  GeV and appears stronger in  $^3\text{He}$ , *i.e.*  $\approx 0.6$ . Qualitatively, these data are consistent with conclusions drawn from earlier work on DIS. There is no experimental evidence for a measurable pion excess. The absence of a measurable excess presents a major challenge to the conventional model of nuclear forces. Work on several fronts is necessary to make further progress in attacking this problem. A precise interpretation of the results presented here will require detailed theoretical estimates of the contributions expected from the exchange currents in the deuteron and  $^3\text{He}$ .

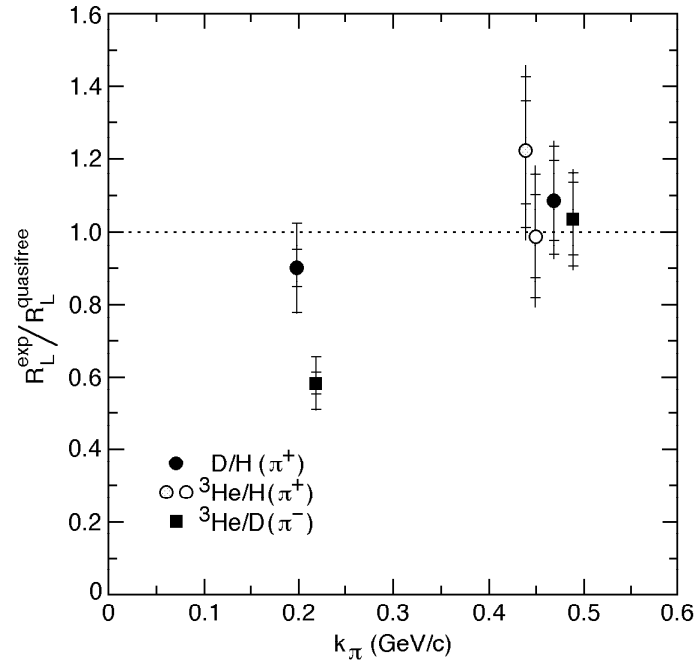


Figure IV-5. The measured ratios of  $d\sigma_l/d\Omega_\pi$  and  $d\sigma_t/d\Omega_\pi$  for single  $\pi^+$  electro-production on the deuteron and  $^3\text{He}$  to the free proton cross section.

**a.10. Pion Electroproduction from H<sub>2</sub> and D<sub>2</sub> at W = 1.95 GeV** (H. E. Jackson, J. Arrington, D. Gaskell, and B. Mueller, and the E93-021 Collaboration)

The pion as the lightest meson, is an ideal system for studying the transition between the non-perturbative and perturbative regions of QCD. Experimental results for the value of the pion form factor, ( $F_\pi$ ), at moderate and high  $Q^2$  have large experimental uncertainties. Experiment E93-021 measured the  $H(e,e'\pi^+)n$  reaction at TJNAF for  $Q^2$  values from 0.6-1.6 (GeV)<sup>2</sup>. Measurements of charged production on the deuteron were also made in the same kinematics to provide additional information on the reaction mechanism. The  $\pi^+/\pi^-$  ratio is sensitive to contributions to the cross section which are unrelated to  $F_\pi$ . The forward longitudinal response in this process is dominated by the pole process and therefore sensitive to the pion form factor. Using the two magnetic spectrometers of Hall C

and electron energies between 2.4 and 4.0 GeV, data for the proton and the deuteron were taken for central values of  $Q^2$  of 0.6, 0.75, 1.0, and 1.6 (GeV/c)<sup>2</sup> at a central value of the invariant mass W of 1.95 GeV. Separated longitudinal and transverse structure functions were measured by means of Rosenbluth separations. New values for the pion charge form factor were extracted from the longitudinal cross section by using a recently developed Regge model. The results indicate that the pion form factor in this region is higher than previously assumed and follows a monopole form factor corresponding to the charge radius of 0.662 fm.

**a.11. Measurement of the Structure Function of the Pion** (R.J. Holt, P.E. Reimer, and K. Wijesooriya)

The light mesons have a central role in nucleon and in nuclear structure. The masses of the lightest hadrons, the mesons, are believed to arise from spontaneous chiral symmetry breaking. The pion, being the lightest meson, is particularly interesting not only because of its importance in chiral perturbation theory, but also because of its importance in explaining the quark sea in the nucleon and the nuclear force in nuclei.

Until recently, the pion structure function was only studied via  $\pi p$  Drell-Yan scattering. New measurements<sup>1</sup> at very low momentum fraction,  $x$ , have been made with semi-inclusive deep inelastic scattering through the process  $ep \rightarrow e'NX$ . In this reaction, the

virtual photon scatters off of the pion in the  $|\pi^+n\rangle$  or  $|\pi^0p\rangle$  or Fock components of the proton and the intact nucleon is detected, as illustrated in Fig. IV-6.

Studies are underway of the feasibility of making such measurements at Jefferson Lab using a 6-GeV incident electron beam using the RAPGAP<sup>2</sup> Monte Carlo program. Early results show that the relatively high luminosity which can be achieved at Jefferson Lab will enable the pion structure to be measured, over a limited range in  $x$ . Additional investigations are being made of this reaction using an upgraded 11-GeV electron beam at Jefferson Lab and using a future  $eA$  collider.<sup>3</sup>

<sup>1</sup>C. Adloff *et al.* (H1 Collaboration), Eur. Phys. J. C **6**, 587 (1999).

<sup>2</sup>H. Jung, Comp. Phys. Commun. **86**, 147 (1995).

<sup>3</sup>R. J. Holt and P. E. Reimer, Proc. Of the Second Workshop on the Polarized Electron Ion Collider, MIT (2000).

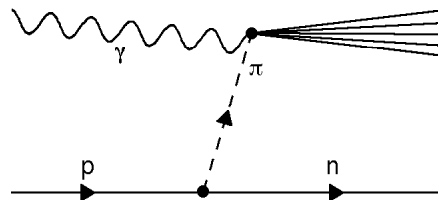


Figure IV-6. Deep inelastic scattering from the pion cloud surrounding a proton.

**a.12. Electroproduction of Kaons and Light Hypernuclei** (J. Arrington, K. Bailey, F. Dohrmann, D. F. Geesaman, K. Hafidi, H. E. Jackson, B. Mueller, T. G. O'Neill, D. Potterveld, P. Reimer, B. Zeidman, and E91-016 Collaboration)

Jefferson Lab experiment E91-016, "Electroproduction of Kaons and Light Hypernuclei" is a study of quasifree production of Kaons on targets of H, D,  $^3\text{He}$ , and  $^4\text{He}$  at an incident electron energy of 3.245 GeV. For H and D targets, data were also obtained at  $E_e = 2.445$  GeV. The scattered electron and emergent  $K^+$  were detected in coincidence with the use of the HMS and SOS spectrometers, respectively, in Hall C. Angular distributions for the  $(e,e'K^+)Y$  reactions were measured at forward angles with respect to the virtual photon for

$Q^2 \approx 0.37$ , and  $0.5 \text{ GeV}^2$ . Particle identification utilizing time-of-flight detectors together with Aerogel Cerenkov detectors yields clean missing mass spectra, e.g. Report ANL/99-12, Fig IV-7, and allows subtraction of random backgrounds. The experiment was run in two time periods. The H and D targets were studied over a period of months near the end of CY 1996 while the balance of the experiment, namely the  $^3,4\text{He}$  targets were investigated during the last few months of CY 1999.

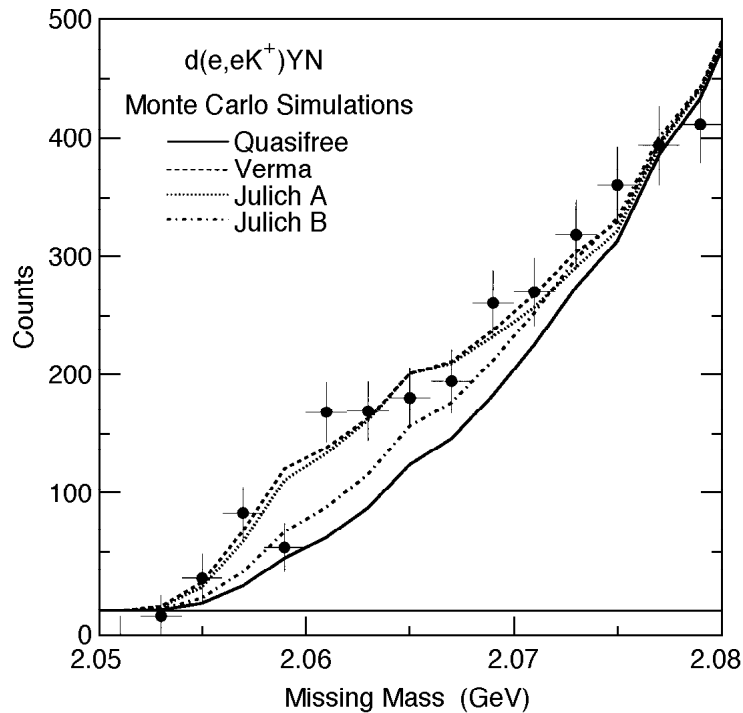


Figure IV-7. Missing mass spectrum for  $D(e,e'K^+)$  near threshold. The lines show Monte Carlo simulations with several  $\Lambda$ - $N$  final state interactions as well as pure quasifree production.

The fundamental interaction being studied is  $N(e,e'K^+)Y$  where  $Y$  is either a  $\Lambda$  or  $\Sigma$  and  $N$  represents a nucleon. For the H target, the final state can only be a  $\Lambda$  or  $\Sigma$ , but for heavier targets, there is relative motion between the nucleons in the target that results in broadening of the peaks. Although it is possible to

separate  $\Lambda$  and  $\Sigma$  contributions for the D target where the Fermi broadening is less than the mass difference between the hyperons, the larger Fermi momenta in the He targets results in greater dependence upon Monte Carlo simulations to extract the various contributions.

Near the threshold for  $\Lambda$  production in the missing mass spectrum for D, *i.e.* the region of low relative momentum in the residual hyperon-neutron system, the interaction of  $\Lambda$  with spectator nucleon leads to an increase of the observed yield relative to pure quasifree production. This final-state-interaction, FSI, has been modeled with three different  $\Lambda$ -nucleon potentials;<sup>1</sup> the results are shown in Fig. IV-7. Two of these potentials describe the data reasonably well despite significant differences in parameterizations so that it is not possible to distinguish them at this time. It is evident, however, that the reaction is sensitive to FSI and a common feature of these potentials is a calculated scattering length of  $\sim -1.6$  fm. Application of the same models to the  $\Sigma$ -N final-state-interaction results in improved agreement with the shape of the spectrum in the region between the quasi-free peaks; the apparent relative strength of the FSI to quasi-free being  $\sim 7$  times greater than for  $\Lambda$ -N.

Because of the greater binding and larger Fermi momenta in  ${}^3\text{He}$  and  ${}^4\text{He}$ , the quasi-free  $\Lambda$  and  $\Sigma$  peaks overlap considerably, complicating the separation of contributions from the various final configurations. While there is no bound  $\Lambda$ -nucleon state, for  ${}^3,4\text{He}$  targets, bound hypernuclear states are known to exist.

Indeed, in Fig. IV-8, there is a clear excess above the quasi-free yield near threshold, but further calculations are required before it will be possible to extract a reliable cross section for the production of the bound  $\Lambda$ -p-n nucleus, *i.e.* the hyper-triton, that is known to have a binding energy of  $\sim 130$  keV. The  $\Lambda$ -N FSI will also contribute near threshold. The bound state is quite evident in the data for  ${}^4\text{He}$  where a state is bound by  $\sim 1$  MeV.

Extraction of cross sections is complicated by the rapidly growing number of final state configurations that must be included in the Monte Carlo simulations with increasing mass. As is seen in Fig IV-8, the present agreement between Monte Carlo simulations and data is not, as yet, satisfactory. Currently, this makes it quite difficult to determine whether bound  $\Sigma^-$  hypernuclear states are indeed observed. There are suggestions of peaks that may exist, but considerably more work is required before definitive answers are available. The present data set provides a high-statistics study of the mass dependence of Kaon electroproduction on light nuclei. Students from Hampton University and the University of Pennsylvania have utilized data from E91-016 for their Ph.D. Theses.

<sup>1</sup>J. Cha, Ph.D. Thesis, Hampton University, Oct. 2000 (unpublished).

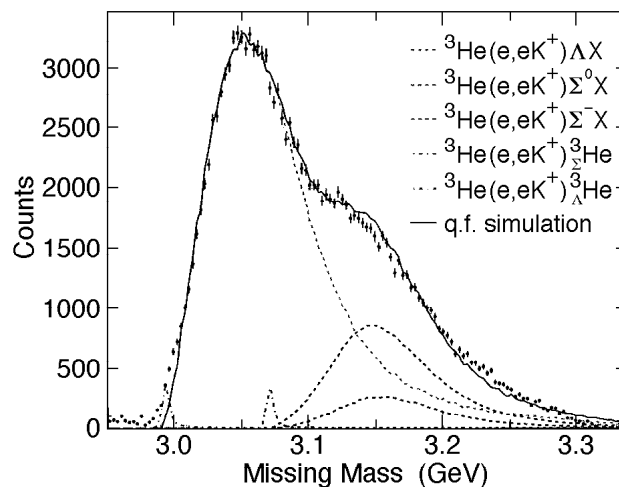


Figure IV-8. Missing mass spectrum for  ${}^3\text{He}(e, e'K^+)YX$ . The various dashed curves represent preliminary Monte Carlo simulations as indicated on the figure. The locations of possible bound  $\Lambda$  and  $\Sigma$  states are indicated by the narrow peaks. The sum of the contributions from the various quasi-free terms is also shown.

### a.13. Measurements of Inclusive Cross Section in the Nucleon Resonance Region

(J. Arrington, D. F. Geesaman, R. Holt, T. G. O'Neill, and D. Potterveld, and the E00-002 and E00-116 Collaborations)

A series of measurements of inclusive electron scattering in the resonance region was performed during in Hall C at Jefferson Lab during 1995 and 1996 running. Data were obtained from both hydrogen and deuterium allowing extraction of the resonance production cross section from both the proton and the neutron. The cross sections were measured<sup>1</sup> for momentum transfers between 0.5 and 5.0 (GeV/c)<sup>2</sup>. An observed scaling relationship between resonance electroproduction and deep inelastic scattering, termed local duality, is generating interest recently. First observed by Bloom and Gilman, this duality suggests a common origin for both kinematic regimes. Local duality was observed both for the entire region and locally in the vicinity of each prominent resonance. In addition, the structure functions measured<sup>2</sup> appear to be insensitive to sea quarks, giving a scaling curve that represents the valence quark distribution of the nucleon. Theoretical models indicate that both the longitudinal and the transverse structure functions should manifest Bloom-Gilman duality, but previous experiments that separated the longitudinal and transverse components did not have the precision necessary to study duality.

There are additional approved experiments to extend duality studies to higher  $Q^2$ , and to study duality in semi-inclusive pion production. These experiments will improve our understanding of duality in inclusive scattering and other reactions. Another approved experiment will to make additional measurements of the proton structure function at low  $x$  and  $Q^2$ , to examine the valence sensitivity of the data and the low  $Q^2$  evolution of the structure functions.

The observation of duality implies that the resonance cross sections can be related to the nucleon (or nuclear) structure functions. This means that it may be possible to measure the structure functions at large values of  $x$  by taking data at moderate  $Q^2$  (in the resonance region), rather than going to very high  $Q^2$  where the cross sections limit the measurements. We have tested this idea by combining data from these resonance region measurement, an  $x > 1$  measurement at Jefferson Lab, and SLAC measurements. By taking data in the resonance region and averaging over a range in  $Q^2$ , we can attempt to extract the structure function in the scaling limit, and then compare this to direct measurement in the DIS region. The same can be done in nuclei, where the Fermi motion on the nucleons performs the necessary averaging. Figure IV-9 shows the ratio of the cross sections for iron and deuterium measured far below the DIS region ( $Q^2 \leq 4 \text{ GeV}^2$ ,  $1.3 < W^2 < 2.8$ ), and see results consistent with measurements of the EMC effect in DIS kinematics ( $Q^2 \geq 5 \text{ GeV}^2$ ,  $W^2 > 4 \text{ GeV}^2$ ). These tests indicate that duality may be a powerful way to access high  $x$  nucleon and nuclear structure, especially as we go to higher beam energies than used in these test cases (4 GeV and below). Results of these studies have been shown at workshops examining the potential of Jefferson Lab at higher energies, and are being written up for publication. Duality studies and the use of duality to access high- $x$  structure make are a significant piece of the physics program for the proposed Jefferson Lab energy upgrade.

<sup>1</sup>I. Niculescu et al., Phys. Rev. Lett. **85**, 1186 (2000).

<sup>2</sup>I. Niculescu et al., Phys. Rev. Lett **85**, 1182 (2000).



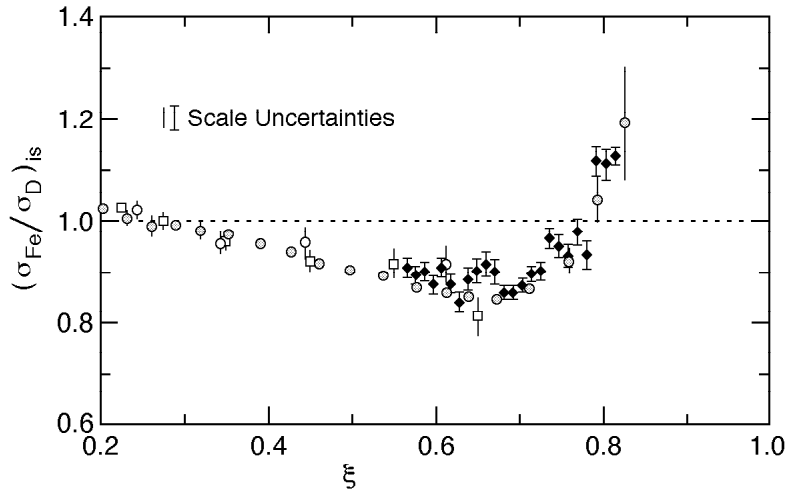


Fig. IV-9. Measurements of the EMC effect for copper and iron, taken in the DIS region, compared to the same measurement taken at Jefferson Lab for  $W^2 < 2.8 \text{ GeV}^2$ . The solid circles (SLAC) and open symbols (CERN) are the DIS measurements. The solid diamonds are the data taken in the resonance region.

#### a.14. Measurements of the Nuclear Dependence of $R = \sigma_L/\sigma_T$ at Low $Q^2$

(J. Arrington, D. F. Geesaman, T. G. O'Neill, and D. Potterveld, and the E99-118 Collaboration)

Inclusive electron scattering is a well understood probe of the partonic structure of nucleons and nuclei. Deep inelastic scattering has been used to make precise measurements of nuclear structure functions over a wide range in  $x$  and  $Q^2$ . The ratio  $R = \sigma_L/\sigma_T$  has been measured reasonably well in deep inelastic scattering at moderate and high  $Q^2$  using hydrogen and deuterium targets. However,  $R$  is still one of the most poorly understood quantities measured in deep inelastic scattering and few measurements exist at low  $Q^2$  or for nuclear targets. Existing data at moderate to large values of  $Q^2$  rule out significant nuclear effects in  $R$ . However, evidence for substantial A-dependent effects has been recently reported by the HERMES collaboration at low  $x$  and  $Q^2$ . While HERMES cannot directly measure  $R$  (which requires data at multiple

beam energies), they do measure the ratio of  $R_A$  to  $R_D$ . They see a significant deviation from unity in the ratio of  $\kappa_{He}/\kappa_D$  and  $R_N/R_D$  for  $x \leq 0.05$  and  $Q^2 \leq 2.0$ .

Jefferson Lab Experiment E99-119 is a direct measurement of  $R$  at low  $x$  (down to  $x = 0.02$ ) and low  $Q^2$  (down to  $0.07 \text{ (GeV/c)}^2$ ). Data were taken on hydrogen, deuterium, aluminum, copper, and gold targets. The hydrogen data will significantly improve the measurement of  $R$  at low  $Q^2$  for the proton, while the data on nuclear targets will be used to examine the nuclear dependence of  $R$  in the region where the HERMES experiments has seen the A-dependence. Experiment E99-119 was run in July of 2000, and the analysis of the data is underway.

**a.15. A Precise Measurement of the Nuclear Dependence of Structure Functions in Light Nuclei** (J. Arrington, F. Dohrmann, D. Gaskell, D. F. Geesaman, K. Hafidi, R. J. Holt, H. E. Jackson, D. H. Potterveld, P. E. Reimer, and B. Zeidman, and the E00-101 Collaboration)

A great deal of effort has gone into attempting to understand the nuclear dependence of the  $F_2$  structure function. The EMC collaboration first measured the difference between the structure function of heavy nuclei and deuterium, indicating a modification of the quark distributions in the nuclear environment. They observed a suppression of the structure function in heavy nuclei at large values of  $x$  (corresponding to large quark momenta), and an enhancement at low  $x$  values. This behavior was termed the 'EMC effect' and has since been measured by several other experiments. Almost all of the existing data is for heavy nuclei ( $A > 8$ ). The ratio of  $F_2$  for the heavy nucleus to  $F_2$  for the deuteron has the same shape for all nuclei, and only the magnitude of the enhancement and suppression depends on the nucleus. Many attempts have been made to explain the EMC effect, but none can fully reproduce the observed modifications, and there is still no consensus on which effect or combination (if any) explains the data.

Experiment E00-101 will measure the EMC effect for  $^3\text{He}$  and  $^4\text{He}$ . The current data cannot distinguish between an  $A$  dependence and a density dependence of the effect. By measuring the EMC effect for light nuclei ( $^3\text{He}$  and  $^4\text{He}$ ) we will extend the range of nuclei for which precision data exists (Fig. IV-10). Because  $^4\text{He}$  has an anomalously large density for a light nucleus, it is the most sensitive test to determine if the EMC effect scales with  $A$  or with nuclear density. More importantly, we will take precision data that can be compared to exact few body calculations. If the EMC effect is caused by few nucleon interactions, the universal shape in heavy nuclei may be a result of a saturation of the effect, and the shape may be different in few-body nuclei. An  $A$ -dependence of the shape of the EMC effect will provide new information we can use to test the proposed explanations of the EMC effect.

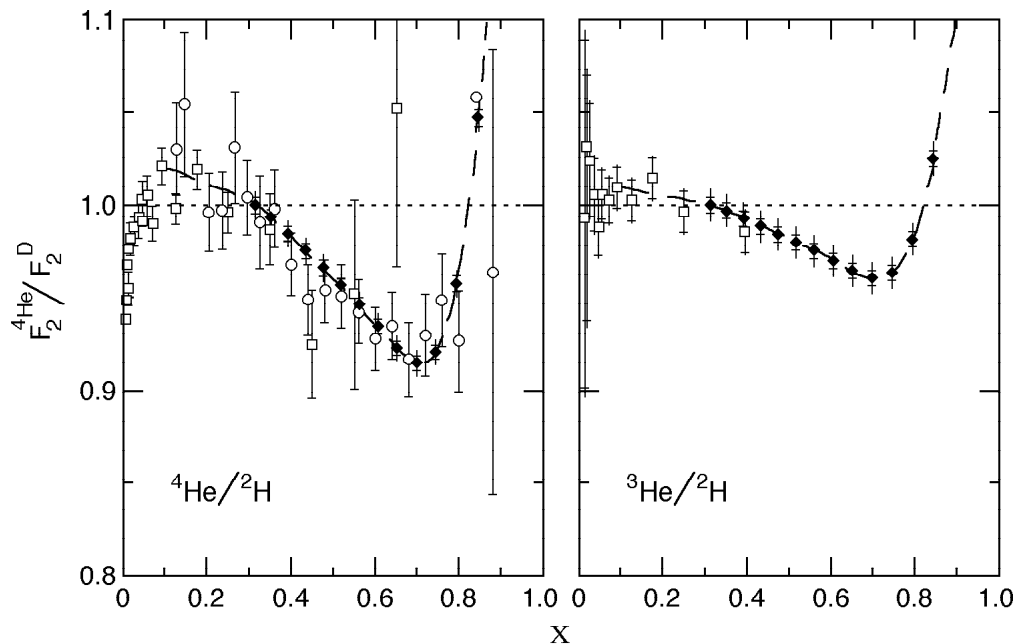


Fig. IV-10. Existing data for the EMC effect in  $^4\text{He}$  and  $^3\text{He}$  (open points), along with projected uncertainties for the approved Jefferson Lab experiment. The existing  $^4\text{He}$  has an additional 2.4% normalization uncertainty (not shown), while the projected uncertainties for  $^4\text{He}$  and  $^3\text{He}$  have a 1.4% normalization uncertainty.

Finally, a measurement of  $A > 4$  nuclei will provide a way to test models of nuclear effects in light nuclei. Models of the nuclear effects in deuterium and  $^3\text{He}$  must be used to extract information on neutron structure, so we need to be able to test and evaluate these models. A high precision measurement including hydrogen, deuterium, helium-3, and helium-4 will give

a single set of data that can be used to evaluate these models in several light nuclei, and help quantify the model dependence of the neutron structure functions inferred from measurements on deuterium and helium-3. A proposal<sup>1</sup> to perform these studies was approved and awarded 10 days of beam time.

<sup>1</sup>J. Arrington et al, JLab Experiment E00-101.

**a.16. HERMES, Measurements of Spin-Structure Functions and Semi-Inclusive Asymmetries for the Proton and Neutron at HERA** (J. Arrington, H. E. Jackson, R. J. Holt, T. G. O'Neill, D. H. Potterveld, P. E. Reimer, D. DeSchepper and K. Hafidi, and collaborators at 33 other institutions)

HERMES, HERA Measurement of Spin, is a second generation experiment to study the spin structure of the nucleon by using polarized internal gas targets in the HERA 30 GeV electron storage ring. Since 1995, the experiment has provided fundamental new insights into the structure of the nucleon and how it is affected by the nuclear medium. The unique capabilities of the experiment have produced data that were not possible with previous measurements at SLAC, CERN, and Fermilab. The collaboration has collected and analyzed millions of deep-inelastic scattering events using longitudinally polarized electrons and positrons incident on longitudinally polarized internal gas targets of  $^1\text{H}$ ,  $^2\text{H}$ , and  $^3\text{He}$ , as well as thicker unpolarized gas targets. These data together with large sets of photo-production events have yielded several results that were unexpected and are provoking new work, both theoretical and experimental.

The primary goal of HERMES is the study of the spin structure of the nucleon. Spin asymmetries have been measured using polarized targets of hydrogen, deuterium, and  $^3\text{He}$ . Analysis of the inclusive and semi-inclusive deep-inelastic scattering data from these unique undiluted targets has resulted in the world's most precise determination to date of the separate contributions of the up, down and sea quarks to the nucleon.<sup>1</sup> Further dramatic improvements are expected from the data recently recorded. One of the surprises yielded by the experiment was a negative polarization asymmetry (though with large statistical uncertainty) in the cross section for photo-production of pairs of hadrons with high transverse momenta, providing the

first direct indication<sup>2</sup> of a positive gluon spin contribution to the nucleon. Again, recent and future data will much improve the statistical precision. Another exciting new result is the observation<sup>3</sup> of a single-spin asymmetry in the azimuthal distribution of positive pions detected in coincidence with the deep-inelastic scattering of positrons from a *longitudinally* polarized proton target. While the theoretical interpretation of this result is under vigorous development, it seems clear that the effect can be explained only by a particular chiral-odd fragmentation function that promises to make feasible at HERMES the first measurement of transversity, the only remaining unmeasured one of the three most fundamental (leading twist) flavour-sets of parton distribution functions. Finally, the most recent and exciting new result from HERMES is the first measurement of a lepton-beam spin asymmetry in the azimuthal distribution of detected photons in Deeply Virtual Compton Scattering (DVCS). Interference with the indistinguishable but well-understood Bethe-Heitler process fortuitously gives rise to a rich variety of such asymmetries, which will continue to emerge from HERMES data. DVCS is considered to be the most reliable of the various hard exclusive processes that constrain the generalized or 'skewed' parton distributions, which are now the subject of intense theoretical development as, *e.g.*, they embody information about *orbital* angular momenta of partons.

The HERMES physics reach extends well beyond nucleon spin structure. The large momentum and solid angle acceptance of the HERMES spectrometer<sup>4</sup> have

opened a much broader range of physics topics to explore, and have truly resulted in a tool for the general study of photon-hadron interactions. Focusing its unique capabilities on specific applications of deep-inelastic scattering (DIS), HERMES has performed a measurement of the flavor asymmetry between up and down quarks in the nucleon sea,<sup>5</sup> several studies of fragmentation of up and down quarks to pions, measurement of the DIS and resonance contributions to the generalized Gerasimov-Drell-Hearn integral for both the proton and neutron,<sup>6,7</sup> a measurement of the spin transfer from virtual photons to  $\Lambda^0$  hyperons,<sup>8</sup> measurements of the effect of the nuclear environment on the hadronization process to study its time development, and recently the observation at small  $Q^2$  of a surprisingly large difference in the effects of the nuclear medium on the transverse and longitudinal DIS cross sections.<sup>9</sup> (Here  $-Q^2 = q^2$  is the square of the invariant mass of the exchanged virtual photon, a measure of the resolution of the probe.) This latter discovery can be interpreted as evidence for nuclear enhancement of mesonic fields, and has inspired further work both at HERMES and elsewhere. A broad program of measurements involving diffractive vector meson production is also underway with basic studies in  $\rho^0$ ,  $\phi$ ,  $\omega$ , and  $J/\psi$  production,<sup>10</sup> as well as the determination of photon $\rightarrow$ vector-meson spin density matrix elements through the analysis of the angular distribution of the decay products.<sup>11</sup> The  $\rho^0$  semi-exclusive cross section has been found to have a large and unexpected spin dependence.<sup>12</sup> The study of diffractive  $\rho^0$  production in nuclei has led to the observation of a lifetime (coherence length) effect on the initial-state nuclear interactions of the virtual quark pair that represent the hadronic structure of the photon, and will lead to new limits on the magnitude of color transparency effects.<sup>13</sup> Some of these results are discussed in more detail below, and references may be found at the end of this report. It is evident that

HERMES has a broad physics program and has a scientific impact on an impressive number of fundamental questions about the strong interaction. HERMES is playing an important role in the worldwide experimental investigation of QCD.

The experiment is technically sound. The means to produce and measure high beam polarization and high target polarization are well understood. The spectrometer and its instrumentation have been carefully modeled and operate reliably and in an understandable fashion. Data analysis software and computational power are now at an advanced stage, allowing the collaboration to produce results in a timely fashion. Furthermore, a vigorous upgrade program has continued to enhance the capabilities of the spectrometer. The gas threshold Cerenkov detector was replaced by a dual-radiator ring-imaging Cerenkov (RICH) detector to identify pions, kaons, and protons over nearly the entire momentum acceptance, and both a new iron wall and the iron of the spectrometer magnet were instrumented to improve the acceptance and identification of high energy muons from charm decay. Finally, preparations are being made for the installation in the first months of 2001 of two new rings of silicon strip detectors just downstream of the target, primarily to enhance the detection of  $\Lambda^0$  decay products. As will be discussed below, the combination of all these new detectors opens the door to new exciting measurements. This extraordinary and unique facility represents the investment of nearly a thousand man-years and 40 MDM, from over 33 institutes from 10 countries in Europe, Asia and North America. Nevertheless, in comparison with other experiments and laboratories, it is highly cost-effective with respect to its productivity and potential.

In the sections which follow a number of recent results of particular interest are discussed.

### 1.1 Inclusive Measurements of the Proton Spin structure Function

Now after many years of work, a series of inclusive scattering experiments at SLAC and CERN as well as HERMES has precisely determined the spin structure functions of both the proton and neutron,  $g_1^p(x)$  and  $g_1^n(x)$  over a range in Björken  $x$  from approximately 0.001 to  $\sim 0.8$ , using various beams, targets and

spectrometers. Results of the measurement of the inclusive spin dependent asymmetry from HERMES, SLAC, and CERN/SMC are shown in Fig. IV-11 where the extracted polarized structure function  $g_1^p(x)$  of the proton is plotted.<sup>14</sup> All three data sets are in remarkable agreement, thus demonstrating that the

experimental uncertainties are well understood. As the SMC data have an average  $Q^2$  that is about a factor of 3 to 10 larger than those of the SLAC and the HERMES measurements, the  $Q^2$  dependence of the asymmetry  $g_1/F_1$  is revealed to be small. Such data have strongly

confirmed the earlier EMC result and extended the range and precision of the knowledge of  $g_1$ , which provides a strong constraint for all models and parameterizations of the polarized quark distributions.

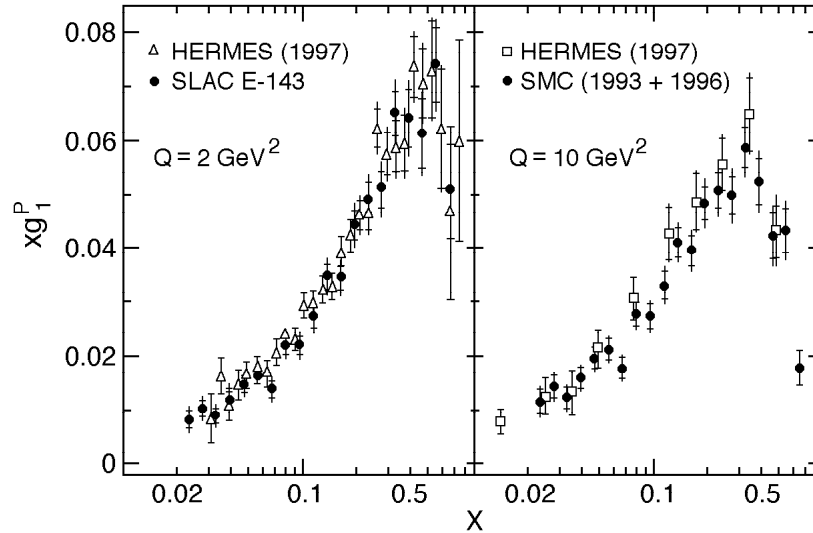


Fig. IV-11. The HERMES measurement of  $g_1^p$  from 1997 data taking compared to SLAC-143 and CERN/SMC. The HERMES data were evolved to the average  $Q^2$  of the other measurements

## 1.2 Flavor decomposition of quark polarization

Information from inclusive scattering is inherently limited by the domination of scattering from up quarks, since the cross sections scale as the square of the electric charge, which is twice as large for up quarks as for down or strange quarks. Also, quarks and antiquarks of the same flavour obviously produce identical effects. To distinguish the contributions of the quark flavors and in particular of the sea quarks, it is necessary to use other types of experimental information. In semi-inclusive scattering, a leading hadron is detected in coincidence with the deep-inelastic scattering of a lepton. The essential principle behind this method is the likelihood of the leading hadron to ‘contain’ the quark originally struck by the virtual photon from the lepton. Scattering asymmetries with various leading hadrons in the final state can be analyzed to determine the fractional contributions of the various quark flavors to the nucleon spin.

With the addition of the RICH detector to the HERMES spectrometer in 1998, the experiment has an

unprecedented ability to directly determine the polarization of the various quark flavor components of the nucleon by measuring semi-inclusive asymmetries with identified leading pions and kaons, in contrast to existing analyses in which the hadronic species were not separated. This lack of separation led to a lack of sensitivity as well as a greater dependence on fragmentation models. Even without hadronic species identification, up quark dominance in DIS has allowed a rather precise determination of  $\Delta u(x)$  by HERMES, using data from the polarized  $^3\text{He}$  and  $^1\text{H}$  targets. The same analysis applied to the deuterium data acquired in 1999/2000 will allow a determination of both  $\Delta u$  and  $\Delta d$  with a precision limited only by systematic uncertainties. The additional capability of identifying pions and kaons will essentially allow us to separate the contribution of the light sea components  $\Delta \bar{u}$  and  $\Delta \bar{d}$  from that of the strange quark sea  $\Delta s$  (assumed equal to  $\Delta \bar{s}$ ). Figure IV-12a displays the projected accuracy of the HERMES determination from the integrated luminosity on deuterium up to the 2000 shutdown,

calculated with parameterizations of Ref. 15. Figure IV-12b shows the online determination of the asymmetry for positive hadrons from this data set. Integrated over the measured region, we should be able to make the first separation of the light and strange sea

contributions, with accuracies that are only systematic in the integral of the light sea quark distribution  $\Delta u_{\text{sea}} + \Delta u + \Delta d_{\text{sea}} + \Delta \bar{d}$  and 0.03 (statistical) in the strange sea ( $\Delta S + \Delta \bar{S}$ ).

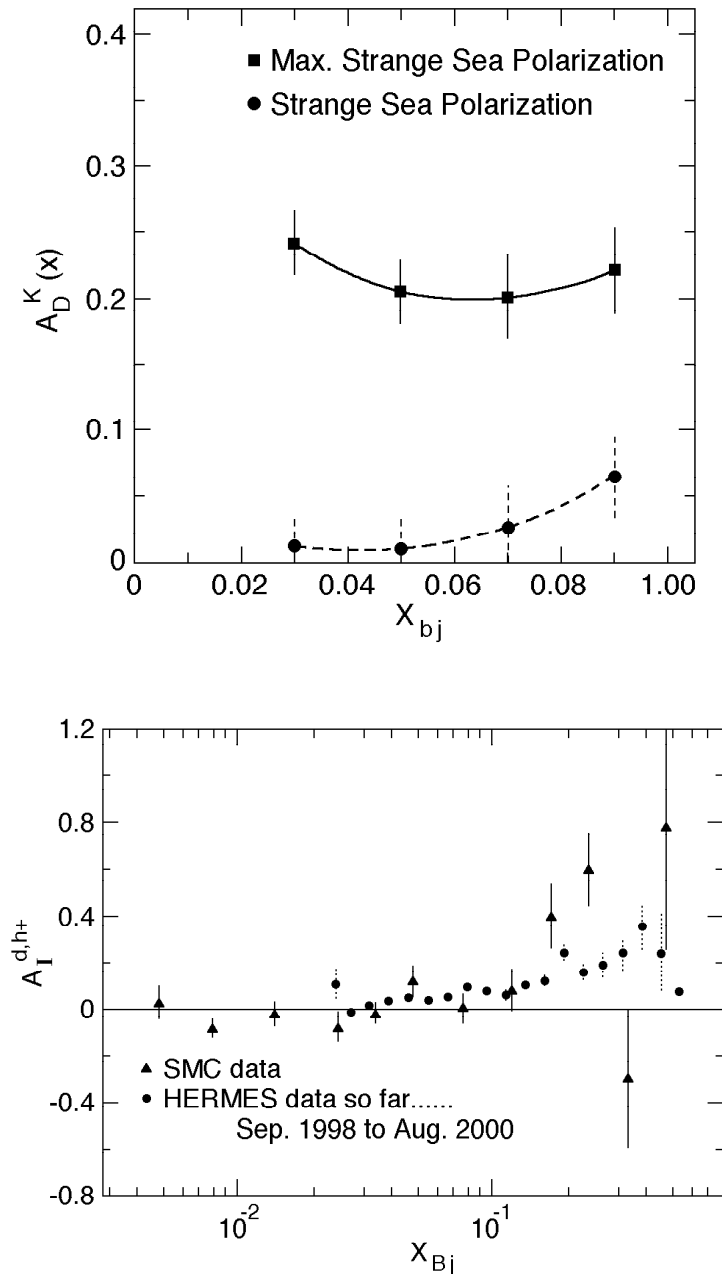


Figure IV-12. a) Predictions showing the expected accuracy of the kaon asymmetry used to determine  $\Delta s$  for the data recorded up to the end of 2000. B) Illustration of the dramatic improvement in quality of semi-inclusive data from the 1999-2000 HERMES data set—asymmetries for positive hadrons.

### 1.3 Gluon polarization

A measurement of the polarization of the gluons in the nucleon is of central importance to understanding the origin of the spin of the nucleon. A promising prospect is a direct measurement of  $\Delta G(x)$  using scattering processes in which the gluon enters in leading order. Such a lepto-production process is photon-gluon fusion (PGF). Experimental signatures of this process are charm production and the production of jets (hadrons) with high transverse momentum. Both of these signals have been successfully exploited at higher energy in measurements of the unpolarized gluon structure function. Such measurements are central goals of the COMPASS experiment<sup>16</sup> at CERN and of the RHIC-SPIN groups in the experiments STAR and PHENIX.<sup>17</sup> At HERMES the spin asymmetry in the polarized photo-production of pairs of hadrons with opposite charge and high transverse momentum has been studied.<sup>2</sup> Under certain kinematical conditions, this signal is dominated by PGF, which has a strong negative polarization analyzing power.

Figure IV-13a presents the measured asymmetry for the highest transverse momenta accessible at HERMES. For  $h^+ h^-$  pairs with  $p_T^{h^+} > 1.5$  GeV/c and  $p_T^{h^-} > 1.0$

GeV/c, the asymmetry is found to be  $A_{\parallel} = -0.28 \pm 0.12$  (stat)  $\pm 0.02$  (sys). This negative value is in contrast to the positive asymmetries typically measured in deep-inelastic scattering from protons, and in the absence of any background process known to give a negative asymmetry, indicates a significant positive gluon polarization. When these data are interpreted in a LO QCD model implemented in the PYTHIA Monte Carlo generator, a value for  $\Delta G(x)/G(x)$  of  $0.41 \pm 0.18 \pm 0.03$  has been determined at  $\langle x_G \rangle = 0.17$ . This result is compared in Fig. IV-13b with several phenomenological LO QCD fits to the data on  $g_1(x, Q^2)$ . No contribution from model uncertainty is included – it requires further study. This information on the gluon polarization from HERMES at relatively low energies was unanticipated. The 1999/2000 polarized *deuteron* data sample is now being examined for a similar asymmetry. The expected ratio of PGF to background is different and the statistical precision of the entire data set will improve considerably. A statistical improvement by a factor of almost 2 is expected already from the 1999/2000 data, as shown by the inner error bars in Fig. IV-13b.

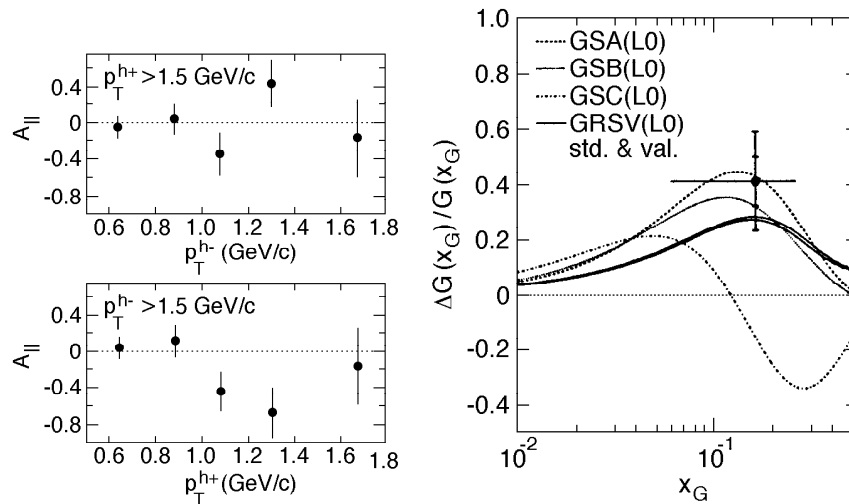


Figure IV-13. a)  $A_{\parallel}(p_T^{h^+}, p_T^{h^-})$  for  $p_T^{h^+} > 1.5$  GeV/c (top) and for  $p_T^{h^-} > 1.5$  GeV/c (bottom). Note that the rightmost data point is identical in both plots. b) The extracted value of  $\Delta G(x)/G(x)$  compared with phenomenological QCD fits to a subset of the world's data on  $g_1^{p,n}(x, Q^2)$ . The curves are evaluated at a scale of 2 (GeV/c)<sup>2</sup>. The indicated error represents statistical and experimental systematic uncertainties only; no theoretical uncertainty is included. The inner error bars indicate the improvement in statistical precision that is expected from an addition 10 Million DIS events on a polarized deuteron target after the luminosity upgrade.

### 1.4 The transversity distribution: a new window on the proton

The complete description of the parton distributions of the nucleon in leading twist (leading order in  $\Lambda_{\text{QCD}}$ ) requires three sets of distributions: the unpolarized distributions contained in  $F_1(x)$ , the helicity distributions contained in  $g_1(x)$  and the still-unmeasured transversity distributions  $\delta q(x)$ , whose structure function will here be denoted as  $h_1(x)$ . Physically, one may think of transversity as the distribution of quarks polarized parallel to the nucleon spin minus the distribution of quarks polarized antiparallel to the nucleon spin, in analogy to the longitudinal case of  $g_1$  except that now the polarization of the nucleon is transverse to its (infinite) momentum, rather than parallel. In a non-relativistic quark model, this is just a simple rotation, and in fact such models predict  $h_1 = g_1$ . However, non-relativistic quark models predict  $g_A/g_V = 5/3$ , in conflict with reality ( $g_A/g_V \cong 1.26$ ). Hence differences between  $h_1$  and  $g_1$  can be expected from relativistic effects in the quark bound state.

A leading-twist fragmentation function that couples conveniently with transversity is known as the Collins function,<sup>18</sup> which is sensitive to the transverse polarization of the struck quark. Until recently, little was known of how large this Collins function might be.

Transversity is expected to have typically large effects in semi-inclusive measurements on a transversely polarized target, but no such effect has yet been clearly seen. Much smaller transversity-related effects based on the same Collins fragmentation function are expected with a *longitudinally* polarized target. Using such a target, HERMES has recently reported the first observation of a single-spin asymmetry in the azimuthal distribution of hadrons detected in coincidence with deep-inelastic lepton scattering (see Fig. IV-14).<sup>3</sup> The sinusoidal target-related spin asymmetry corresponds to an analyzing power of  $0.022 \pm 0.005$  (stat)  $\pm 0.003$  (sys) for positive pions, and is consistent with zero for negative pions. It has been found<sup>19</sup> that these data are consistent with models for the relevant distribution functions together with a model for the Collins fragmentation function that is also consistent with a preliminary value for this function from  $Z^0 \rightarrow 2\text{-jet}$  decay.<sup>20</sup> Hence it appears that the Collins fragmentation function is responsible for the effect and has a substantial value, thus opening the way to future measurements of transversity using transversely polarized targets. The proposed measurement of  $h_1$  at HERMES would yield a fundamentally new type of information about nucleon structure, as did the first measurements of  $F_1$  and  $g_1$  decades ago.

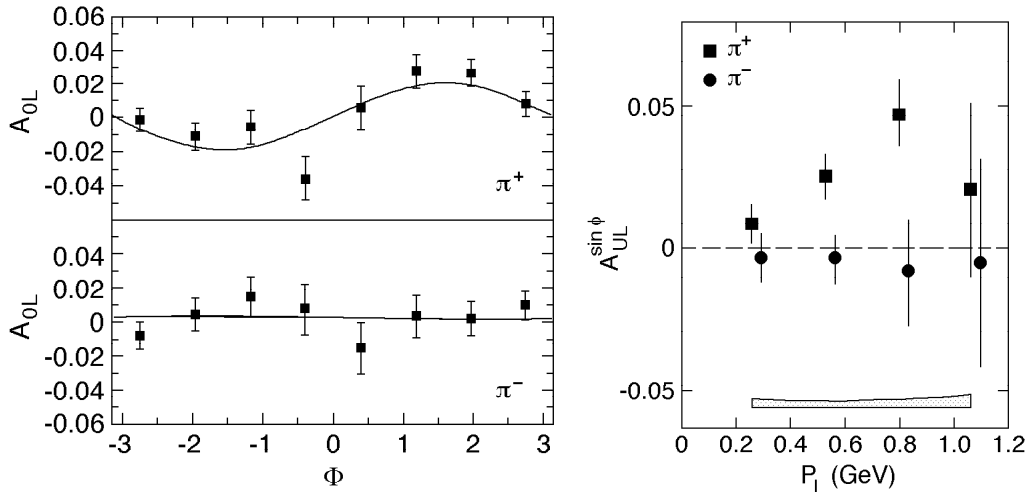


Figure IV-14. a) The azimuthal asymmetry for positive and negative pions measured on a longitudinally polarized proton target at HERMES, and b) target-spin analyzing powers in the  $\sin \phi$  moment as a function of transverse momentum, for  $\pi^+$  (squares) and  $\pi^-$  (circles). Error bars show statistical uncertainties and the band represents the systematic uncertainties.



### 1.5 Measurements with unpolarized targets-Hadron formation times

HERMES has an active program in measurements with unpolarized targets which addresses a range of topics in photon-hadron interactions. As an example, HERMES has measured the charged pion fragmentation functions for up and down quarks from the nucleon, and their attenuation in a nuclear environment. By embedding the fragmentation process in the nuclear medium, one can study the time propagation of the hadron formation process. The attenuation of hadrons, which is measured as a function of the energy transfer  $\nu$  and the hadron energy fraction  $z = E_h/\nu$ , can be related to the formation length (or time) of the hadron, or can be compared directly to model calculations describing the interaction of a color string with the surrounding medium. In fact, such data can also be used to derive empirical values for the hadron formation time and the energy loss of a quark propagating in the medium. These quantities are of considerable theoretical<sup>21</sup> and experimental interest, as it is possible to apply the same concepts in the description of the Drell-Yan process and heavy-ion collisions.<sup>22</sup>

Preliminary HERMES results for the attenuation ratio of pion production in nitrogen compared to deuterium are shown in Fig. IV-15a. The observed effect increases with decreasing energy transfer  $\nu$ , and also at large  $z$  as observed here for the first time. These precise data can distinguish between different models describing fragmentation in a nuclear environment. As the RICH had not been installed at that time, no definitive distinction could be made between formation times of pions, kaons and protons. However, comparison of results from negative hadrons with those of positive ones that receive a substantial contribution from protons suggest that proton formation times are longer than those of pions. It is very desirable to obtain more data for separate hadrons in the future, as the possible mass dependence of the formation time is a distinctive feature of the available models. It is also important to carry out the analysis on 2 or 3 different nuclei in order to ensure that the resulting formation times are independent of  $A$ , as expected. The projected accuracies of the ratios for kaons and pions together with the required running times for  $^{14}\text{N}$ ,  $^{40}\text{Ar}$ ,  $^{84}\text{Kr}$  and  $^{131}\text{Xe}$  are shown in Fig. IV-15b.

<sup>1</sup>K. Ackerstaff *et al.*, Phys. Lett. B **464**, 123 (1999).

<sup>2</sup>A. Airapetian *et al.*, DESY 99-071; Phys. Rev. Lett. **84**, 2584 (2000).

<sup>3</sup>A. Airapetian *et al.*, DESY 99-149; Phys. Rev. Lett. **84**, 4047 (2000).

<sup>4</sup>K. Ackerstaff *et al.*, Nucl. Instr. and Meth. A **417**, 230 (1998).

<sup>5</sup>K. Ackerstaff *et al.*, Phys. Rev. Lett. **81**, 5519 (1998).

<sup>6</sup>K. Ackerstaff *et al.*, Phys. Lett. B **444**, 531, (1998).

<sup>7</sup>A. Airapetian *et al.*, DESY 00-096, hep-ex/0008037.

<sup>8</sup>A. Airapetian *et al.*, DESY 99-151, hep-ex/9911017.

<sup>9</sup>K. Ackerstaff *et al.*, DESY 99-150, Phys. Lett. B **475**, 386 (2000).

<sup>10</sup>A. Airapetian *et al.*, hep-ex/0004023, accepted by Eur. Phys. J. C

<sup>11</sup>K. Ackerstaff *et al.*, DESY 99-199, hep-ex/0002016.

<sup>12</sup>F. Meissner, Proceedings of the 7<sup>th</sup> International Workshop on Deep Inelastic Scattering and QCD, Zeuthen, Germany, April 1999 (NEED PAGE NUMBERS)

<sup>13</sup>K. Ackerstaff *et al.*, Phys. Rev. Lett. **82**, 3025 (1999).

<sup>14</sup>A. Airapetian *et al.*, Phys. Lett. B **442**, 484 (1998).

<sup>15</sup>M. Gück *et al.*, Phys. Rev. D **53**, 4775 (1996).

<sup>16</sup>The COMPSS Collaboration, CERN/SPSLC 96-14 (1996).

<sup>17</sup>S. E. Vigdor *et al.*, hep-ex/9905034.

<sup>18</sup>J. C. Collins, Nucl. Phys. B **396**, 161 (1993).

<sup>19</sup>A. M. Kotzinian *et al.*, hep-ph/9908466.

<sup>20</sup>A. V. Efremov, O. G. Smirnova, and L. G. Tkachev, Nucl. Phys. Proc. Suppl. **74**, 49 (1999).

<sup>21</sup>R. Baier *et al.*, Nucl. Phys. B **483**, 291 (1997); *ibid* B **484**, 261 (1997).

<sup>22</sup>B. Kopeliovich, A. Schaefer, and A. Tarasov, Phys. Rev. C **59**, 609 (1999).

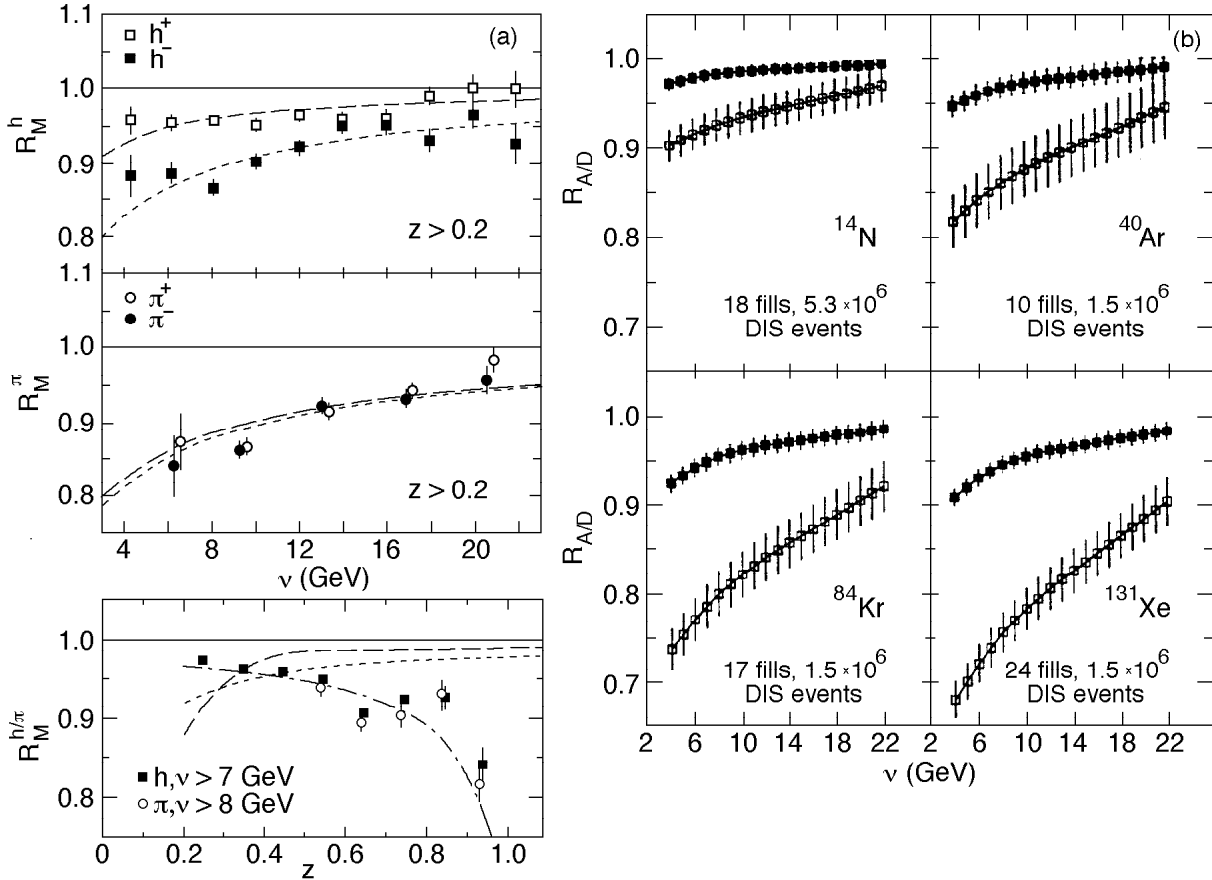


Figure IV-15. a) The measured attenuation of hadron multiplicities in a nuclear environment, compared to predictions of the gluon-bremsstrahlung model (dashed-dot) or various parameterizations in terms of hadron formation times, and b) Projections for measurements of the attenuation of pion (filled symbols) and kaon (open symbols) multiplicities from DIS in various nuclei. See text for details.

**a.17. A Dual Radiator Ring Imaging Cerenkov Counter for HERMES** (H. E. Jackson, K. G. Bailey, D. M. DeSchepper, T. P. O'Connor, T. G. O'Neill, and D. H. Potterveld, and the HERMES Colloration)

Unambiguous identification of pions, kaons, and protons is essential for the HERMES experiment, a study of the spin structure of the nucleon carried out using the HERA accelerator at DESY, Hamburg. The HERMES program emphasizes measurements of semi-inclusive deep-inelastic scattering. Previously, limited particle identification was provided by means of threshold Cerenkov counters. Recently, these counters were replaced with dual-radiator ring-imaging Cerenkov counters (RICH) which employ a new technology. The detectors were designed and built by a collaboration of

8 institutions, led by Argonne (Argonne, BARI, CalTech, Frascati, Gent, Rome, Tokyo, and Zuethen). They provide particle identification for pions, kaons, and protons in the momentum range from 2 to 15 GeV, which is essential to these studies. The instrument uses two radiators,  $\text{C}_4\text{F}_{10}$ , a heavy fluorocarbon gas, and a wall of silica aerogel tiles. The use of aerogel in a RICH detector has only recently become possible as a result of the development of clear, large, homogeneous and hydrophobic aerogel. A lightweight mirror was constructed using a newly perfected technique to make

resin-coated carbon-fiber surfaces of optical quality. The photon detector consists of 1934 photomultiplier tubes (PMT) for each detector half, held in a soft steel matrix to provide shielding against the residual field of the main spectrometer magnet.

For a fully relativistic particle, a typical ring pattern on the focal plane consists of a small inner ring generated by photons from the gas and a larger concentric ring generated by photons from the aerogel. The radii of the rings correspond to the specific angles at which the Cerenkov photons are emitted along the particle tracks. The Cerenkov angles produced by the combination of the aerogel and gas radiators for tracks corresponding to pions, kaons, and protons are plotted in Fig. IV-16 together with a scatter plot of angles actually measured for particles transversing the

HERMES spectrometer. This plot demonstrates the essential features of the system which provide the particle identification.

The HERMES RICH has been operating routinely as part of the experiment since its installation. Its operation has been stable and reliable for more than two years. The single photon angular resolution for ideal tracks is close to the expected values. The particle identification based on inverse ray-tracing has been implemented and its likelihood analysis has been optimized. More elaborate particle identification procedures are under development. The performance has met the design goals. Hadron identification by the RICH detector will be a crucial feature of the analysis of current and future HERMES data.

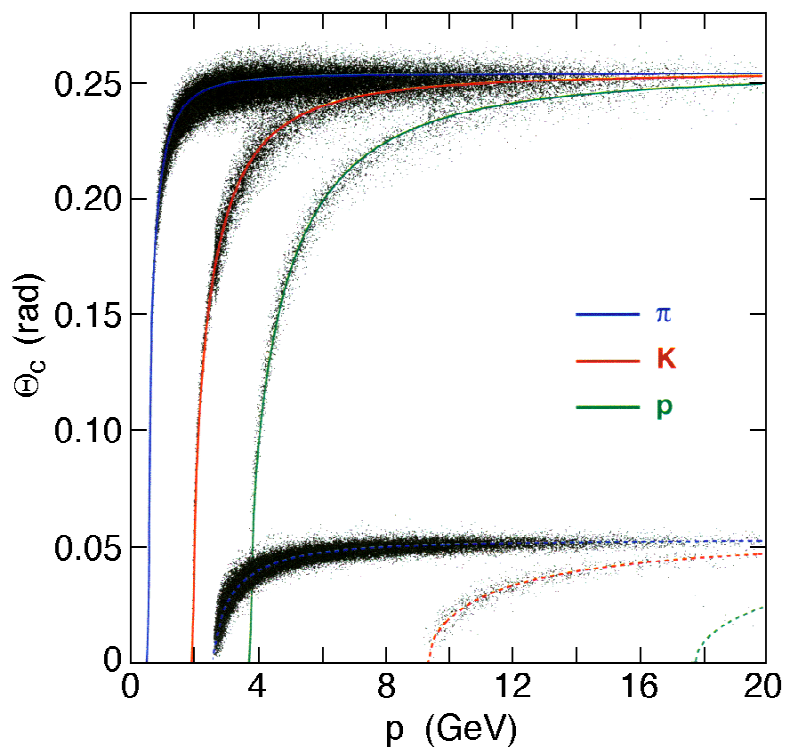


Figure IV-16. The Cerenkov angle  $\theta$  versus hadron momentum for the aerogel and  $C_4F_{10}$  gas radiators.

**a.18. An Exploration of the Antiquark Sea of the Proton Using Drell-Yan Scattering**  
(D. F. Geesaman, S. B. Kaufman, N. Makins, B. A. Mueller, and P. E. Reimer and the FNAL E866/NuSea collaboration)

While it is not required by any fundamental symmetry, it has – until recently – been widely assumed that distributions of anti-down ( $\bar{d}$ ) and anti-up ( $\bar{u}$ ) quarks in the proton sea were identical. This assumption was based on the belief the the proton's sea arose perturbatively from gluon splitting into quark–anti-quark pairs. Since the mass difference between the up and down quarks is small, equal numbers of up and down pairs should result. Recent evidence from Deep Inelastic Scattering (DIS), however, showed that there is an integral difference between the anti-up and anti-down distributions. To further explore this difference, the Fermilab 866/NuSea experiment measured the ratio of  $\bar{d}/\bar{u}$  as a function of the momentum carried by the struck quark,  $x$ . Data were collected in 1996-1997 using the Meson East Spectrometer at Fermilab by measuring Drell-Yan produced muon pairs produced by bombarding 800 GeV protons on hydrogen and deuterium targets. Measurements of the nuclear dependence of  $J/\psi$ ,  $\psi'$  and Drell-Yan production were made using Be, Fe and W targets were also made.

The full analysis of the hydrogen and deuterium data is now complete. From the ratio of deuterium to

hydrogen Drell-Yan cross sections, the ratio  $\bar{d}/\bar{u}$  and the difference  $\bar{d}-\bar{u}$  have been extracted. This revealed a striking,  $x$ -dependent asymmetry in the proton's anti-quark sea, which was not expected. The flavor difference is a pure flavor non-singlet quantity: its integral is  $Q^2$  independent and its  $Q^2$  evolution, at leading order, does not depend on the gluon distributions in the proton. The large differences seen in Fig. IV-17 must be non-perturbative in nature. Several approaches have been suggested to produce this difference, which include 1) hardonic model so the meson cloud of the nucleon,<sup>1</sup> 2) chiral quarks models which couple mesons directly to the constituent quarks,<sup>2</sup> and 3) instanton models.<sup>3</sup> These are illustrated by the curves in Fig. IV-17.

Absolute Drell-Yan cross sections are also being extracted from the hydrogen and deuterium data. To next-to-leading order in  $\alpha_s$ , this cross section is easily calculated and can be compared directly with data. While the ratio was sensitive to the relative strength of the different flavors of anti-quarks, the absolute cross section is sensitive to the total strength of the anti-quark sea,  $\bar{d} + \bar{u}$ .

<sup>1</sup>FNAL E866/NuSea Collaboration, J. C. Peng *et al.*, Phys. Rev. D **58**, 092004 (1998); FNAL E866/NuSea

Collaboration, R. S. Towell *et al.*, in preparation; N. N. Nikolaev *et al.*, Phys. Rev. D **60**, 014004 (1999).

<sup>2</sup>A. Szczurek *et al.*, J. Phys. G: Nucl. Part. Phys. **22**, 1741 (1996); P. V. Pobylitsa *et al.*, Phys. Rev. D **59**, 034024 (1999).

<sup>3</sup>A. E. Dorokhov and N. I. Kochelev, Phys. Lett. B **259**, 335 (1991); Phys. Lett. B **304**, 167 (1993).

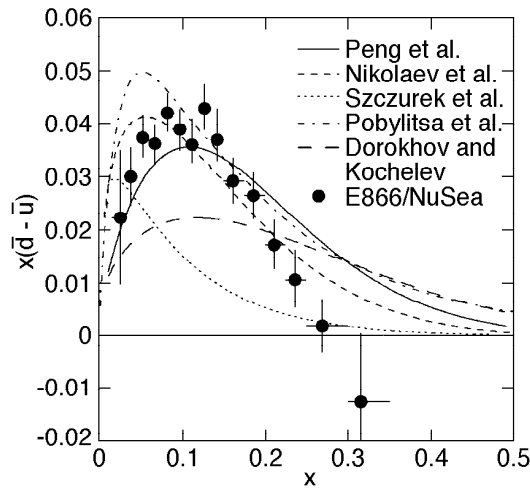


Figure IV-17. The  $x$ -dependence of the difference  $x(\bar{d}-\bar{u})$  of the proton at a mass scale of 7.353 GeV. The curves represent several model calculations as described in the text.

**a.19. Nuclear Dependence of Lepton Pair Production: Parton Energy Loss, Shadowing and  $J/\psi$  and  $\psi'$  Suppression** (D. F. Geesaman, S. B. Kaufman, N. Makins, B. A. Mueller, P. E. Reimer and the FNAL E866/NuSea Collaboration)

Through comparisons of production cross sections from nuclear targets, we can deduce information about the behavior of quarks in a strongly interacting environment and learn how nuclear size affects the production processes. FNAL E866/NuSea collected Drell-Yan,  $J/\psi$  and  $\psi'$  data using Beryllium, Iron and Tungsten targets.

One phenomena studied was nuclear shadowing. Shadowing, although not well understood, is seen and well parameterized from Deep Inelastic Scattering experiments. It is also expected to be present in Drell-Yan lepton pair production. By comparing the Drell-Yan yields from nuclear targets we were able to confirm that shadowing in Drell-Yan quantitatively matches predictions based on shadowing in DIS. In the Drell-Yan process, the colored initial-state quarks interact strongly as they pass through the nucleus. After the interaction, the final state muons, however, do not interact significantly in the nuclear medium. This,

combined with the ability to quantitatively correct for nuclear shadowing, makes Drell-Yan an ideal tool for the study of quark energy loss in the initial state. Using the same data, corrected for shadowing, very tight limits were placed on the energy loss of partons traveling through cold nuclear matter.

Although not well explained, the rate of production of the  $J/\psi$  and  $\psi'$  is diminished in nuclear targets relative to the same process with a proton target. Using nuclear targets, E866/NuSea is studying this suppression as a function of the kinematics variables Feynman- $x$  ( $x_F$ ) and transverse momentum. One significant observation, as shown in Fig. IV-18, is a difference in suppression of the  $J/\psi$  and  $\psi'$  at low values of  $x_F$ , where the  $\psi'$  is suppressed more than the  $J/\psi$ . This affect might be attributable to the absorption of the  $c\bar{c}$  pair in the nucleus before hadronization. Other effects, such as shadowing, also play important roles in the observed suppression.

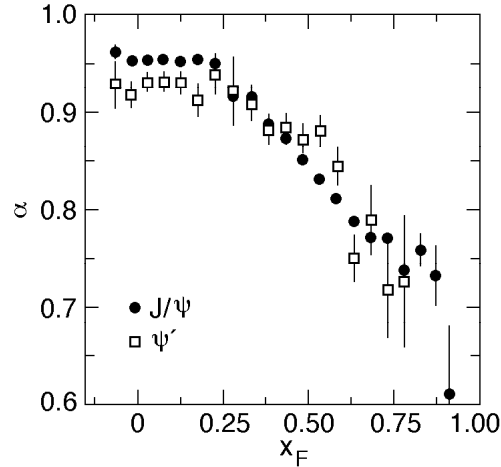


Figure IV-18. Nuclear suppression of  $\psi$  and  $\psi'$  production parameterized in terms of  $\alpha$  where  $\sigma_A = \sigma_p A^\alpha$  and  $\sigma_A$ ,  $\sigma_p$  represent the production cross section on a nuclear target and a free proton, respectively.

**a.20. Production of  $\Upsilon$  and  $J/\psi$  from 800-GeV Protons Incident on  $D_2$  and  $H_2$  Targets**  
(D.F. Geesaman, S.B. Kaufman, N. Makins, B.A. Mueller, P.E. Reimer and the FNAL E866/NuSea Collaboration)

Although the primary motivation for E866 was to detect dimuon events generated in Drell-Yan reactions, the detector is sensitive to any process which produces pairs of muons. One such process is heavy quark vector meson production.  $\Upsilon$  and  $J/\psi$  particles are produced when partons from the beam and target annihilate and form a virtual gluon which then hadronizes into a heavy resonance state. The virtual gluon which produce the resonance can be generated by the annihilation of either a quark/antiquark pair or a pair of gluons. Resonance production is therefore sensitive to both the quark and gluon distributions within the beam and target.  $J/\psi$  production is believed to occur dominantly via gluon-gluon fusion, while  $\Upsilon$  production is thought to have contributions from both gluon-gluon fusion and quark-antiquark annihilation. Because the gluon distribution for the proton and neutron are thought to be the same, the per nucleon  $J/\psi$  production cross section is expected to be the same for hydrogen and deuterium. The  $\Upsilon$  production ratio, on the other hand, is expected to be larger than unity since  $\bar{u}^N > \bar{u}^p$  for the values of fractional momentum,  $x$ , probed by FNAL E866/NuSea.

The E866 hydrogen and deuterium data samples contain approximately 30 thousand  $\Upsilon$  and 1 million  $J/\psi$  events. The cross sections values, extracted by fitting the mass spectra of the data, can be compared to predictions based on models and parton distributions available in the literature. Color evaporation model (CEM) calculations have been performed for both  $J/\psi$  and  $\Upsilon$  production from  $H_2$  and  $D_2$ . Although the CEM model is extremely simple and cannot predict the absolute value of the cross sections, the  $x$ -Feynman shape is reproduced by the CEM calculation. Further, the unknown scale factor in the CEM calculations cancels when the  $D_2/H_2$  per-nucleon ratio is calculated. The extracted cross section ratio,  $\sigma^D/2\sigma^H$ , for  $J/\psi$  and  $\Upsilon$  production are shown in Fig. IV-19. The  $J/\psi$  ratio is close to unity, which is consistent with expectations assuming gluon fusion production. The  $\Upsilon$  ratio is also consistent with unity, which is in disagreement with the CEM calculation when either the MRST or CTEQ5M parton distribution functions (PDFs) are used. The deviation from the prediction may indicate that the PDFs underestimate the hard gluon ( $x \approx 0.25$ ) distribution in the proton.

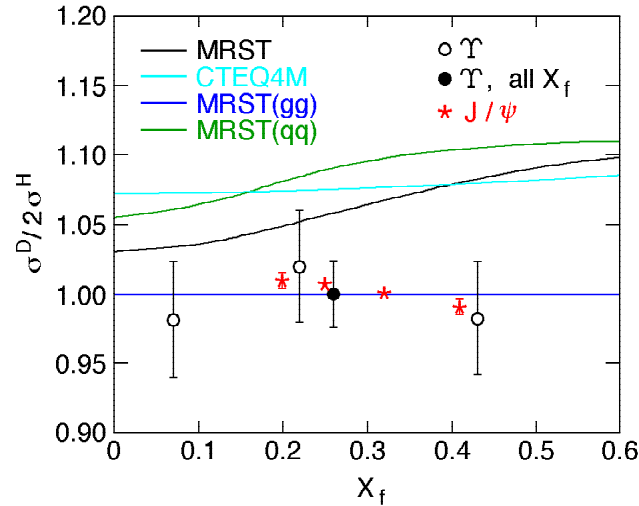


Figure IV-19. The data points show the ratio of cross sections for  $\Upsilon$  and  $J/\psi$  production from deuterium and hydrogen. The curves correspond to color evaporation model calculations using several different parameterizations for the nucleon parton distributions.

#### a.21. Polarization Measurements of $\Upsilon$ and $\psi$ Production in Proton-Nucleus Collisions (D. F. Geesaman, S. B. Kaufman, N. Makins, B. A. Mueller, and P. E. Reimer and the FNAL E866/NuSea Collaboration)

Despite QCD's overwhelming success in describing many aspects of the strong interaction, an adequate description of quarkonia production is still lacking, due, in part, to its non-perturbative nature. Various models of quarkonia production have been proposed, including the Color Octet model, and these models make predictions for polarization in quarkonia production. Due to the clean signature provided by their lepton pair decay mode, the  $\Upsilon$  and  $\psi$  meson families provide an important system in which to study this. FNAL E866/NuSea has measured the polarization of quarkonia in the  $\psi$  and  $\Upsilon$  families.

In data from FNAL E866, the  $\Upsilon(1S)$  is seen to exhibit only a slight polarization, and that only at large  $x$ -Feynman ( $x_F$ ) or large transverse momenta ( $p_T$ ). The observed  $\Upsilon(1S)$  signal, however contains not only direct production of  $\Upsilon$ 's but also  $\Upsilon$ 's produced indirectly

through decays of higher mass  $b\bar{b}$  states. Due to their higher masses, there exist fewer states which can feed the  $\Upsilon(2S)$  and  $(3S)$  states, so their polarization better reflects the polarization inherent in the production mechanism. FNAL E866/NuSea observes near complete transverse polarization in these two states (unresolved) as shown in Fig. IV-20.

In the  $\psi$  family, the observed  $J/\psi$ 's show only a slight polarization, which changes from transverse to longitudinal as a function of  $x_F$ . Once again, however, the polarization signal from direct production is diluted by feed down from other  $c\bar{c}$  states. Data on the polarization of the  $\psi'$  is currently under analysis. While statistics are limited, so that the functional dependence cannot be determined, this state has the advantage that the entire signal is from direct production.

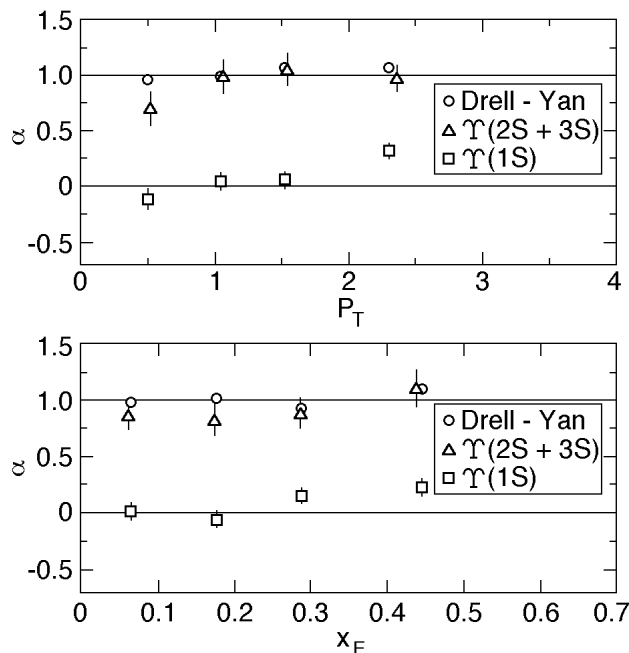


Figure IV-20. The observed polarization of  $\Upsilon(1S)$  and unresolved  $\Upsilon(2S)$  and  $\Upsilon(3S)$  production as a function of a)  $x_F$  and (b)  $p_T$ . A value of  $\alpha = 1$  represents complete transverse polarization, while  $\alpha = 0$  is unpolarized. The Drell-Yan polarization is also shown, which is expected to be completely transversely polarized.

**a.22. Lepton Pair Production with 120-GeV Protons to Extend the Measurement of  $\bar{d}/\bar{u}$  in the Nucleon** (D. F. Geesaman, R. J. Holt, D. H. Potterveld, P. E. Reimer, L. D. Isenhower,\* M. E. Sadler,\* C.N. Brown,† G.T. Garvey,‡ M. J. Leitch,‡ P. L. McGaughey,‡ J.-C. Peng,‡ R. Gilman,§ C. Glashauser,§ X. Jiang,§ R. Ransome,§ S. Strauch,§ C. A. Gagliardi,¶ R. E. Tribble,¶ M. A. Vasiliev,¶ and D. D. Koetke||)

The measurement by the Fermilab 866/NuSea Experiment revealed an unexpected dependence of the  $\bar{d}/\bar{u}$  ratio on the momentum fraction of the struck quark,  $x$ . For  $x > 0.19$  the antiquark asymmetry began to decline, returning to a completely symmetric sea near the highest values of  $x$  accessible to the experiment – a striking difference from what was expected based on parameterizations available prior to the 866/NuSea measurement. A significant extension of the  $x$ -range can be achieved with a higher-intensity, lower-energy beam, making this a study ideally suited for a “slow extraction” beam from the 120 GeV Fermilab main injector. The expected statistical errors which could be obtained from such a measurement are shown in Fig. IV-21.

After a favorably received letter-of-intent, a full proposal for this measurement was submitted to Fermilab in the spring of 1999. At that time, the Fermilab decided not to commit to a fixed target program based on a slow extraction because of its effect on the collider luminosity and the time scales of the other experiments which were proposed for this type of beam. The collaboration was encouraged to submit a proposal in the spring of 2001 when the impact of a fixed target program will be reconsidered. The collaboration intends to resubmit a new proposal at this time, and we are actively working toward this end.

\*Abilene Christian University; †Fermi National Accelerator Laboratory; ‡Los Alamos National Laboratory; §Rutgers University; ¶Texas A&M University; ||Valparaiso University



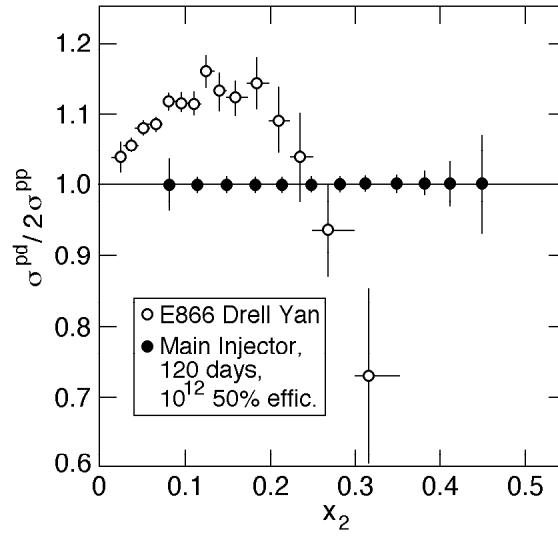


Fig. IV-21. Expected statistical precision for the proposed experiment (error bars with solid circles) arbitrarily plotted at a ratio of 1.0. Systematic errors are estimated to be less than 1%. Also shown are the Fermilab E866/NuSea results (open circles) for the  $x$ -dependence of the ratio of Drell-Yan cross sections from deuterium and hydrogen.

## B. ATOM TRAP TRACE ANALYSIS

### b.1. Building a Practical ATTA system for $^{81}\text{Kr}$ -Dating (K. Bailey, C. Y. Chen, X. Du, Y. M. Li, Z.-T. Lu, T. P. O'Connor, L. Young,\* and G. Winkler†-)

We are improving our atom-counting system with the goal of realizing  $^{81}\text{Kr}$ -dating of ancient groundwater and polar ice. Our system is based on Atom Trap Trace Analysis (ATTA),<sup>1</sup> a new method of ultrasensitive trace-isotope analysis. ATTA has been used to count individual  $^{85}\text{Kr}$  ( $t_{1/2} = 10.8$  yr) and  $^{81}\text{Kr}$  ( $t_{1/2} = 2 \times 10^5$  yr) atoms present in a natural krypton gas sample with isotopic abundances in the range of  $10^{-11}$  and  $10^{-13}$ , respectively. The counting efficiency demonstrated in 1999 was  $2 \times 10^{-7}$ . For practical applications, such as  $^{81}\text{Kr}$ -dating of ancient groundwater or polar ice, a much higher efficiency ( $10^{-4}$ - $10^{-3}$ ) is required.

In 2000, we implemented several improvements to the atomic beam system for an increased counting efficiency and counting rate.<sup>2</sup> A RF-driven discharge is used to produce a beam of metastable krypton atoms at the  $5s[3/2]_2$  level with the angular flux density of  $4 \times 10^{14} \text{ s}^{-1}\text{sr}^{-1}$  and the most-probable velocity of 290 m/s, while consuming  $7 \times 10^{16}$  krypton atoms/s (see Fig.

IV-22). When operated in a gas-recirculation mode, the consumption is reduced to  $2 \times 10^{15}$  krypton atoms/s with the same atomic-beam output. By combining this new recirculating source with the atom counter, we expect to improve the counting rate by one order of magnitude, and the counting efficiency by two orders of magnitude. Further improvements to sample recirculation are being developed, which should result in an even greater increase in counting efficiency.

We have also replaced the Ti:Sapphire ring laser system with an array of diode lasers. The diode laser system offers long-term stability while requiring less maintenance. A new frequency control system is under construction. When completed, the system will be able to switch every minute between counting  $^{81}\text{Kr}$  and counting reference Kr isotopes, thereby allowing the cancellation of some common-mode systematic errors in the measurements of isotopic abundance.

\*Chemistry Division, ANL; †University of Vienna, Vienna, Austria

<sup>1</sup>C.Y. Chen *et al.*, *Science* **286**, 1139 (1999).

<sup>2</sup>C.Y. Chen *et al.*, *Rev. Sci. Instr.* **72**, 271 (2001).

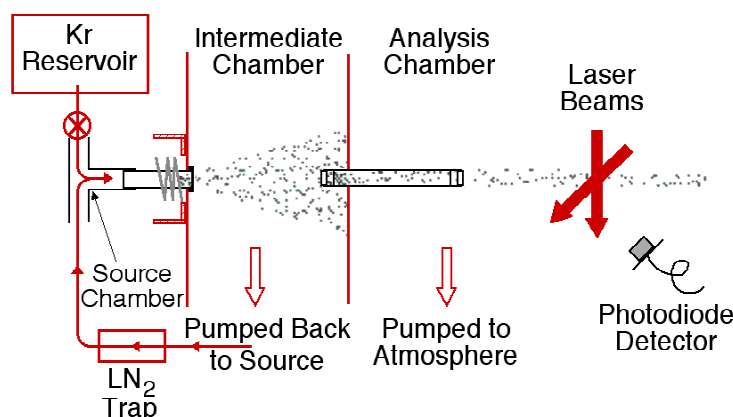


Figure IV-22. Schematic of the RF-driven discharge source and the diagnostics setup. Kr gas flows through a discharge region that fills the inside of a glass tube. The discharge is driven by a coaxial RF resonator. For recirculation, the gas in the intermediate chamber is pumped back to the source chamber. The atomic beam flux and velocity distribution are determined using laser spectroscopy techniques.

### b.2. Atom Trap Trace Analysis of $^{41}\text{Ca}$ (K. Bailey, X. Du, Y. M. Li, Z.-T. Lu, T. P. O'Connor, and L. Young\*)

Calcium is an essential element in both biological and geological objects. In particular, its presence in human bones has motivated us to develop a  $^{41}\text{Ca}$  ( $t_{1/2} = 103$  kyr) analyzer, based on the new Atom Trap Trace Analysis (ATTA) method,<sup>1</sup> for important applications in biomedical research and archaeology. For archaeological dating, an analyzer is required to detect  $^{41}\text{Ca}$  in natural bone samples at the isotopic abundance level of  $10^{-14}$ . The task is much easier for bio-medical applications since the isotopic abundance of artificially introduced  $^{41}\text{Ca}$  can be as high as  $10^{-9}$ .

In 2000, we have built an atom-trap system (Fig. IV-23), and succeeded in trapping and detecting all stable

calcium isotopes (Fig. IV-24). The demonstrated capture rate of the abundant  $^{40}\text{Ca}$  (isotopic abundance = 96.94%) was  $3 \times 10^{10} \text{ s}^{-1}$  and the capture efficiency was approximately  $1 \times 10^{-4}$ . These performance parameters are already sufficient for the analyses of  $^{41}\text{Ca}$  in natural bone samples. For example, a 10% measurement would require 3 days and a calcium sample of about 10 mg. At present, we are developing the capability of detecting a single trapped atom, which is a necessary step towards the analysis of  $^{41}\text{Ca}$ . We are also improving the source design and incorporating a transverse cooling scheme for an increased counting rate and counting efficiency.

\*Chemistry Division, ANL

<sup>1</sup>C.Y. Chen *et al.*, Science **286**, 1139 (1999).

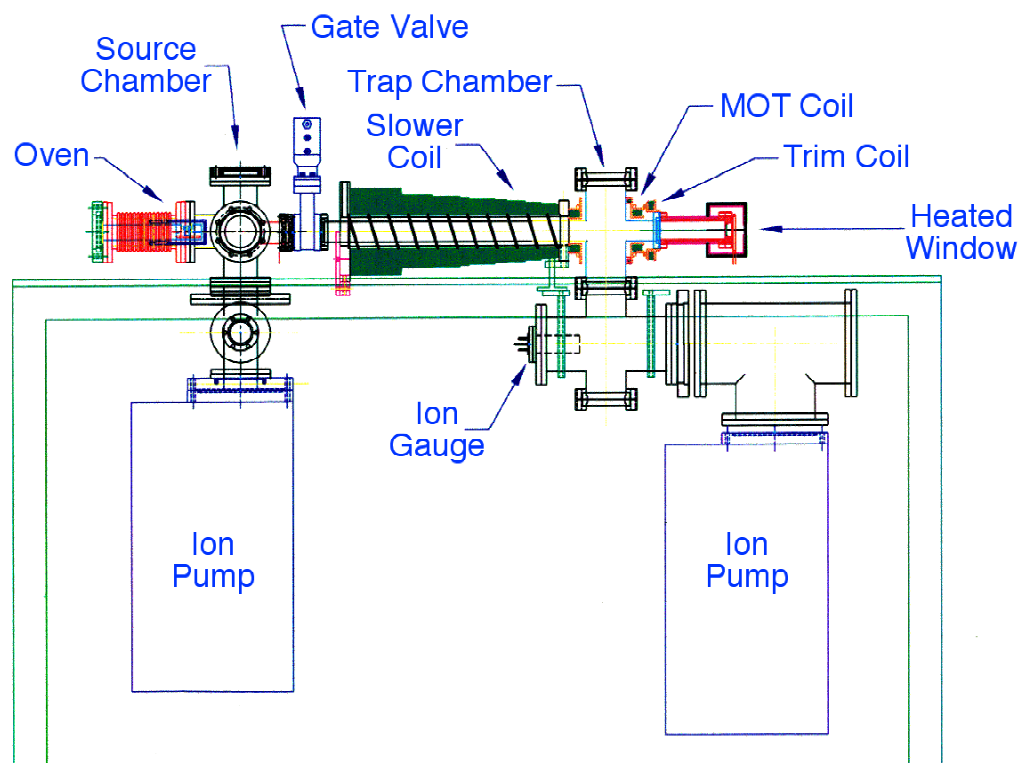


Figure IV-23. A schematic of the atomic beam system. A collimated beam of Ca atoms is produced by a heated oven. Atoms are then slowed down in a Zeeman slower and captured by a magneto-optical trap. The fluorescence of the trapped atoms is measured, based on which the number of trapped atoms is deduced.

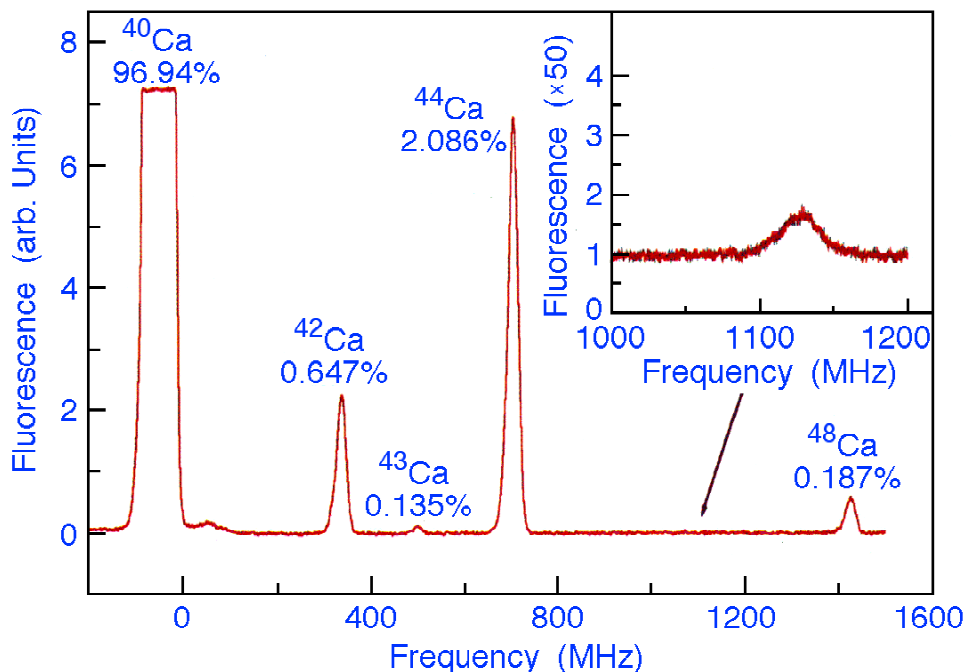


Figure IV-24. The fluorescence signal from laser trapped calcium atoms. Atoms of different isotopes are trapped at different laser frequencies due to isotope shifts. The detector used here is set in photo-current mode. Its gain is 50 times higher when detecting the least abundant  $^{46}\text{Ca}$  (0.004%) than the gain used in detecting other Ca isotopes. In order to detect  $^{41}\text{Ca}$ , a different detector, set in photon-counting mode, will be used in place of the current detector.

**b.3. Measuring the Charge Radius of  $^6\text{He}$**  (Z.-T. Lu, K. E. Rehm, K. Bailey, J. A. Caggiano, P. Collon, X. Du, A. M. Heinz, R. V. F. Janssens, C.-L. Jiang, Y. M. Li, T. P. O'Connor, R. C. Pardo, J. P. Schiffer, and M. Paul\*)

The neutron-rich  $^6\text{He}$  ( $t_{1/2} = 807$  ms) nucleus consists of a  $^4\text{He}$ -like core and two halo neutrons bound by less than 1 MeV. Such low binding in a light nucleus offers a unique opportunity to compare the properties of such a nucleus with the "Nuclear Standard Model," the first successful attempt to calculate nuclear properties from the interactions between free nucleons for  $A > 4$ .  $^6\text{He}$  is expected to differ from  $^4\text{He}$  in charge radius, partly because the motion of the center of mass of the core with respect to the halo nucleons. A precision measurement of the charge radius will probe the wavefunction of this nucleus. The Quantum-Monte-Carlo calculations, based on the Argonne V18 Two-Nucleon and the Illinois Three-Nucleon Potential, have enabled a precise prediction of the charge radius of  $^6\text{He}$  ( $1.89 \pm 0.01$  fm).<sup>1</sup> The proposed measurement would test this theory in a region away from nuclear stability.

We propose to determine the charge radius of  $^6\text{He}$  by measuring the atomic isotope shift of the  $2^3\text{S}_1$ - $2^3\text{P}_2$  transition between  $^4\text{He}$  and  $^6\text{He}$ . If the isotope shift is measured to a precision of 10%, or  $\sim 100$  kHz, then the charge radius of  $^6\text{He}$  can be determined to 2%. Since  $^6\text{He}$  atoms are short-lived and are available only in small numbers, we propose to use the ATTA method and perform precision laser spectroscopy on trapped metastable  $^6\text{He}$  atoms. As a test, we obtained spectroscopy with the ATTA method on the rare  $^{85}\text{Kr}$  (isotopic abundance  $\sim 1 \times 10^{-11}$ ) atoms at a flow rate of  $1 \times 10^5$   $^{85}\text{Kr}/\text{s}$ .<sup>2</sup>

We plan to produce and extract neutral  $^6\text{He}$  atoms at ATLAS. In this scheme,  $^6\text{He}$  atoms are produced via the  $^9\text{Be}(^7\text{Li}, ^6\text{He})^{10}\text{B}$  reaction in a thick beryllium target that can be heated to 1300C. The  $^6\text{He}$  atoms thermalize in and then diffuse out of the heated target as neutral

atoms. With an energy-averaged cross section of 1 mb and a beam intensity of 500 pnA, one calculates a production yield of  $10^7$   $^6\text{He}$  /s.

In 2000, A target and extraction system has been designed, and the construction of this system is currently underway. Experiments to test the production

and extraction of  $^6\text{He}$  atoms have been approved by an ATLAS PAC and are scheduled to run in early 2001. Meanwhile, a laser laboratory that consists of an optical table and all the amenities to meet safety requirements has been established. A diode laser and an optical system for the laser spectroscopy of helium atoms is under development.

---

\*Hebrew University

<sup>1</sup>B.S. Pudliner, V.R. Pandharipande, J. Carlson, S. C. Pieper, and R. B. Wiringa, Phys. Rev. C **56**, 1720 (1997).

<sup>2</sup>C.Y. Chen *et al.*, Science **286**, 1139 (1999).

#### **b.4. Feasibility Study for Atomic Parity Violation Measurements in the Hydrogen Isotopes** (R. J. Holt, D. H. Beck,\* J. G. Eden,\* Z. Lu,\* E. Thorsland,\* J. White,\* and L.-B. Wang\*)

Atomic parity violation experiments<sup>1</sup> can provide a very sensitive test of the standard model. Measurements for the hydrogen isotopes are highly desirable because of the relative simplicity of the theoretical calculations. One of the central limitations of previous experiments to measure parity violation for the hydrogen atom is the use of fast (500 eV) metastable hydrogen beams. These fast atoms traveling in a magnetic field induce a motional electric field which leads to a large systematic error. The goal of this feasibility study is to determine whether an intense *thermal* beam of metastable hydrogen atoms can be

produced using recent advances in VUV laser technology. Thus far, a beam of more than  $10^{10}$  metastable H atoms/s has been produced by two-photon excitation. This result represents an advance of four orders of magnitude for optical production of metastable H atoms. An advance of at least two more orders of magnitude would be necessary for an atomic parity violation experiment. Work is continuing in collaboration with the University of Illinois at Urbana-Champaign to determine whether a substantial increase in the yield can be produced.

---

\*University of Illinois, Urbana-Champaign

<sup>1</sup>C. S. Wood *et al.*, Science **275**, 1759 1997.

